FINITE ELEMENT ANALYSIS OF STRAIN DISTRIBUTION ON A PDMS MEMBRANE

WALEED JEHAD MOHAMMAD ODEIBAT

JUNE 2023

ÇANKAYA UNIVERSITY

GRADUATE SCHOOL OF NATURAL AND APPLIED SCIENCES

DEPARTMENT OF MECHANICAL ENGINEERING

M.SC. THESIS IN

MECHANICAL ENGINEERING

FINITE ELEMENT ANALYSIS OF STRAIN DISTRIBUTION ON A PDMS MEMBRANE

WALEED JEHAD MOHAMMAD ODEIBAT

JUNE 2023

ABSTRACT

FINITE ELEMENT ANALYSIS OF STRAIN DISTRIBUTION ON A PDMS MEMBRANE

Odeibat, Waleed Jehad Mohammad

M.Sc. in Mechanical Engineering

Supervisor: Associate Prof. Dr. Samet Akar

Co-Supervisor: Prof. Dr. Pervin Rukiye DINÇER

June 2023, 80 pages

Mechanotransduction and mechanosensing are two main mechanisms by which the cells respond when exposed to mechanical stimuli. These types of cellular responses can be investigated using dedicated cell stretching devices. However, strain uniformity which greatly affects the collected data's accuracy and reliability is the main challenge when using these devices. In this thesis, a polydimethylsiloxane (PDMS) membrane with uniform strain distribution has been designed and fabricated. Parametric finite element analysis (FEA) has optimized the membrane's size and shape. The FEA study is performed by modeling the problem as a displacement-controlled problem, where strains up to 20% have been examined. Hole diameter, membrane thickness, chamfer length, and sidewall thickness are the parameters that are optimized. A uniformity index of 90 % has been achieved, equivalent to an 80% improvement compared to commercial membranes. Suitable hyperelastic material model parameters are calculated to model the nonlinear behavior of the membrane materials under uniaxial tension. A five-parameter Mooney-Rivlin material model is shown to be the most suitable material model when compared to the experimental data. The issues related to the failure of the membranes have been solved by tailoring material properties by changing the ratio of the cross-linker to the base material and

curing time and temperature. A PDMS with a ratio of 0.75:10 cured at 60°C for four hours fulfills the cell stretching requirements.

Key Words: Polydimethylsiloxane, Finite Element Analysis, Membrane, Tailoring, Hyperelastic.

ÖZET

BIR PDMS MEMBRANDA GERINIM DAĞILIMININ SONLU ELEMANLAR ANALIZI

Odeibat, Waleed Jehad Mohammad
Makine Mühendisliği Yüksek Lisans

Danışman: Assistant Prof. Dr. Samet Akar
Ortak Danışman: Prof. Dr. Pervin Rukiye DINÇER
Haziran 2023, 80 sayfa

Mechanotransdüksiyon (mekanik iletim) ve mekanoduyarlılık(mekanik duyarlılık) , hücrelerin mekanik uyarılara maruz kaldığında yanıt verdiği iki temel mekanizmadır. Bu tür hücresel yanıtlar, özel hücre gerdirme cihazları kullanılarak incelenebilir. Bununla birlikte, verilerin doğruluğunu ve güvenilirliğini büyük ölçüde etkileyen gerilim homojenliğinin sağlanması, bu cihazların kullanımında karşılaşılan temel zorluktur. Bu tezde, homojen gerilim dağılımına sahip bir polidimetilsiloksan (PDMS) membran tasarlanmış ve üretilmiştir. Parametrik sonlu eleman analizi (SEA) ile membranın boyutları ve şekli optimize edilmiştir. SEA çalışmasında, sorun gerilimlerin %20'ye kadar incelendiği durumu simüle eden bir yer değiştirme kontrollü problem olarak modellenmiştir. Delik çapı, membran kalınlığı, yuvarlak kenar uzunluğu ve yan duvar kalınlığı değişkenlerinin iyileştirilmesi üzerinde çalışılmıştır. Ticari membranlara göre %80 iyileşme ile eşdeğer olduğu düşünülebilecek %90' lık bir homojenlik indeksi elde edilmiştir. Tek eksenli gerilim altında membran malzemesinin doğrusal olmayan davranışını modellemek için uygun hiper elastik malzeme model parametreleri hesaplanmıştır. Beş parametreli Mooney-Rivlin malzeme modeli, deneysel verilerle karşılaştırıldığında en uygun malzeme modeli olarak belirlenmiştir. Membranları başarısız kılan nedenler, çapraz

bağlayıcının baz malzemeye oranının ve sertleşme süresi ile sıcaklığının değiştirilmesi ve sonuçta malzeme özelliklerinin ayarlanmasıyla çözülmüştür. 0.75:10 oranında 60°C'de dört saat süreyle sertleştirilen PDMS' in, hücre germe gereksinimlerini karşıladığı ortaya konmuştur.

Anahtar Kelimeler: Sonlu Eleman Analizi, Membran, Hiper Elastik, Polidimetilsiloksan.

ACKNOWLEDGEMENT

Firstly all praise goes to ALLAH who enabled and gave me the opportunity to finish this thesis successfully. I would like to express my sincere gratitude to my parents for their unconditional support and sacrifice to me. Your memories would ever shine in my mind. Also, I would like to thank Mousa TAMARI player of Montpellier and Jordanian national team for giving motivation and honor.

Special thanks to my supervisor Assistant Prof. Dr. Samet AKAR for the guidance through my study period and his help which without it couldn't be possible to conduct this research and to the Scientific and Technological Research Council of Türkiye (TÜBİTAK) for their support. Also, my special gratitude goes to the head of mechanical engineering department Prof. Dr. Haşmet TÜRKOĞLU and to the rest of the thesis committee Asst. Prof. Dr. Şehram DİZECİ and Asst. Prof. Dr. Ferit SAİT for the encouragement and insightful comments.

TABLE OF CONTENTS

LIST OF TABLES

LIST OF FIGURES

LIST OF SYMBOLS AND ABBREVIATIONS

SYMBOLS

MPa	:Megapascal
GPa	:Gigapascal
nm	:Nanometer
µm	:Micrometer
mm	:Millimeter
N	:Newton
°C	:Degrees Celsius
U	:Strain energy function

ABBREVIATIONS

FEA	:Finite Element Analysis
PDMS	:Polydimethylsiloxane
ASTM	:American Society for Testing and Materials
RPM	:Revolutions per minute
SE	:Silicone Elastomer
METU	:Middle East Technical University
CNC	:Computer Numerical Control
UTS	:Ultimate Tensile Strength

CHAPTER I

INTRODUCTION

1.1 BACKGROUND

Human cells interact under deformation and these interactions affect cells behavior, and as long as human and any living cell is concerned it's important to know how they behave under these conditions. It's crucial to deal with such a subject that holds heavy consequences without studying the nature of it and here comes the importance of this study. Under stress, cells tend to change significantly under a microscopic scale, but the amount of stress and its mechanism of conveying the stress should be controlled so the desired outcome can be obtained. Previous studies show that when cells are stretched, the cells respond by relocating themselves to avoid stress (Boynton et al. 2019: 10). By studying cellular responses to stress, mechanobiologists can give an overview of cellular behavior. By comprehending the mechanisms through which mechanical forces trigger molecular, cellular, and tissue-level alterations, the field of mechanobiology offers valuable insights into tissue physiology and the progression of diseases. Moreover, it presents novel perspectives for the development of therapeutic strategies with clinical relevance.

Polydimethylsiloxane (PDMS) belongs to a group of polymeric organosilicon compounds that are considered as silicon is used in this study, a thin membrane made out of Sylgard-184 PDMS will be the transfer medium which will deliver the stresses that are applied on the membrane to the cells placed above it.

1.2 THESIS AIM

This study aims to design a membrane that has a high strain uniformity when stretched, different membranes are designed each of which has a distinct geometry that strain dissipates through. Using finite element analysis (FEA) to test each membrane gives the predicted strain behavior. Another important purpose of this work is to examine the concept of how production parameters will impact the final product in

terms of durability during testing. Hardener (cross-linker) to PDMS ratio and curing conditions for the mixture such as temperature and time are all factors that determine strain-stress behavior and failure of the material mainly due to the tearing. Another aspect of the study which is of paramount importance is how to model the nonlinear behavior of the PDMS material. Several material models are available each using a different equation and way to solve that makes each model result different than the other. Even though all material models solve using their relevant formula, each of them gives a solution that may or may not be accurately compared to experimental or real data. By using FEA, material models are tested to know which is the most reliable according to this scope.

The importance of knowing strain and stress on a living cell is that the amount of strain and stresses inside the body differs from tissue to tissue, for example, bone cells are subjected to mechanical loading which has the highest amplitude on the other hand stresses on tissues such as muscle or veins is completely different and its milder than bone cells. Each cell type can tolerate a specific amount of stress according to its 3D shape and its function, so according to mimic cells same conditions must be provided and in this case, the deformation they go through in a human body is simulated on top of the membrane.

1.3 THESIS OUTLINE

This thesis comprises five chapters, each serving a specific purpose in the research investigation. Chapter 1 serves as an introduction, providing a comprehensive background of the subject matter and highlighting the significance of cell stretching and strain uniformity. Additionally, this chapter clearly articulates the aim of the thesis.

Chapter 2 presents a thorough literature review, encompassing the pertinent and previously reported information that is related to cell stretching and challenges in the field. This chapter serves as a foundation for the research, ensuring that the study is built upon existing knowledge and insights.

Chapter 3, the research methodology chapter, details the comprehensive approach undertaken throughout the thesis. A comprehensive explanation of the finite element modeling has been provided along with the proper selection of the material model for the PDMS. Also, the fabrication and testing methods are discussed in detail.

In Chapter 4, the results and outcomes derived from the research conducted in Chapter 3 are extensively discussed. This chapter presents a detailed analysis of the stress and strain distribution and provides valuable insights and interpretations related to the optimum membrane geometry.

Chapter 5, the concluding chapter, offers a concise summary of the key findings and implications drawn from the research. Furthermore, it provides valuable suggestions for future research endeavors, highlighting potential areas of exploration and advancement within the same subject area.

CHAPTER II

LITERATURE REVIEW

2.1 INTRODUCTION

PDMS material specifications and membrane fabrication is discussed widely in previous studies since this area is open for diligence and research that gives a good ground to start from and a pathway of what can be done regarding this subject. Also, virtual testing using simulation software or real laboratory testing of PDMS gives a reliable number of research done that can be helpful for research. This chapter will discuss what has been done in the following areas, which includes:

1- PDMS characteristics, structure, and applications
2- PDMS membrane fabrication
3- Stretching methods and devices
4- Finite element analysis of PDMS membranes and different
5- PDMS to hardener ratio effect

2.2 PDMS CHARACTERISTICS, STRUCTURE AND APPLICATIONS

2.2.1 Characteristics And Structure

Polydimethylsiloxane, also known as PDMS, is a polymer that belongs to the silicon elastomers group (Victor et al. 2019: 2), its empirical formula is C2H6OSi and its fragment formula is CH3[Si(CH3)2O]nSi(CH3)3 as shown in Figure 1 where n is the monomers repetition so depending on the monomers chains the PDMS could be a liquid or thick to semisolid material (Seethapathy and Górecki 2012: 1).

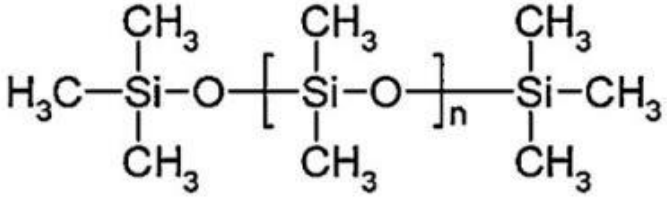

Figure 1: PDMS chemical structure (Seethapathy and Górecki 2012: 1).

PDMS material properties have given it an advantage over other materials such as regular silicon and glass, its good microstructural characteristics, manufacturability, and cost also. PDMS is transparent so it can be easier to detect cells and thermally stable (Victor et al. 2019: 2), also the range of elasticity of PDMS is from 1 MPa to 3 MPa which makes it better in medical applications compared to glass which is around 50 GPa (Miranda et al. 2022: 3). In addition, is environmentally friendly so it doesn't have any negative effect on the environment. The only notable disadvantage may be that it's a hydrophobic material which means that it's hard to wet the surface using aqueous solvents (Victor et al. 2019: 2). Although it's a hydrophobic material it can be easily changed to hydrophilic by applying plasma treatment.

2.2.2 Biocompatibility And Applications

Biocompatibility is the ability of the material to be compatible with biological tissues. It's important to know if the material is so because some materials that may be implanted into living bodies can cause inflammatory response and damage, this response is caused by the immune system aiming the body to fight against these strange materials. Due to this, it's important to find a material that is compatible and does not cause any harm to the body, PDMS is a material that lowers the impact and the interference of tissue response that makes it the most studied implantable polymer. (Victor et al. 2019: 3).

Since its high biocompatibility, the applications of PDMS in medical fields are wide. PDMS can be used in drainage and catheter tubing, microvalves, micro pumps, and optical lenses (Victor et al. 2019: 1). Also using this material can go beyond that so it can mimic living tissues, a recent study showed that PDMS is used as an intracranial aneurysm shown in Figure 2, to model the mechanical behavior of blood vessels and a FEA simulation is done using the numerical values found out by the PDMS mimicking organ (Rodrigues et al. 2016: 263). Also, PDMS allows easy observation of the mimicked blood flow inside the mimicked vessels because of its high transmittance that can reach up to 90% with a wavelength between 390 nm and 780 nm (Miranda et al. 2022: 3).

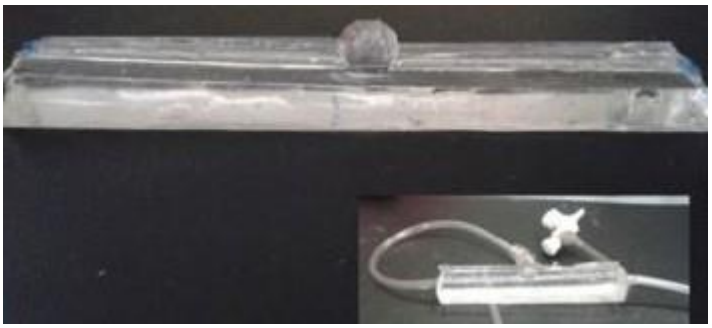

Figure 2: PDMS intracranial aneurysm model (Rodrigues et al. 2016: 264).

2.3 PDMS MEMBRANE FABRICATION

There are several ways for PDMS membrane fabrication, each of which serves a need and they are produced in several ways.

One of the PDMS productions is a specimen that will be used for a tensile test, first, the mixture has a ratio of 1:10 (hardener/PDMS) in grams, the PDMS used here is Sylgard-184, then it's placed into the vacuum for around 20 minutes and poured into the mold according to ASTM-412-C standard which related to tensile test mold for soft materials. The mold is placed in the oven at 80°C for 2 hours (Cho et al. 2021: 2). The Figure 3 bellow shows the specimen after being removed from the oven.

Figure 3: Specimen produced according to ASTM-412-C standard (Cho et al. 2021: 3).

Another method of PDMS membrane production is spin coating. This method uses centripetal force to spread the PDMS mixture on a petri dish. The spin coater RPM controls the thickness of the final membrane, the faster the rotation the thinner the membrane. For example, a rotating spin coater of 500 RPM for 30 seconds results in a membrane of a thickness of around 200 µm, after that the membrane is carefully removed. The spin coater device shown in Figure 4 has a controller for speed and time to produce the membrane thickness needed (Sadegh-Cheri 2019: 1269).

Figure 4: Spin coater device with speed and time controllers (Sadegh-Cheri 2019: 1269).

The thickness of a PDMS membrane can vary depending on the specific application and fabrication method. However, PDMS membranes are commonly fabricated with thicknesses ranging from a few micrometers (μm) to several hundred micrometers. The thickness of a PDMS membrane has several effects on its properties and performance. Listed below are some factors influenced by the thickness of the membrane:

1- Mechanical flexibility: thin membranes tend to be more flexible and deformable than thick membranes. This flexibility is an advantage in applications requiring membrane conformability or elasticity, such as microfluidics or biological sensing.

2- Mechanical strength: thick membranes generally possess higher mechanical strength and rigidity compared to thin membranes. This can be an advantage in applications where membrane durability or resistance under deformation is critical.

3- Sensitivity: in some applications, such as pressure or strain sensing, the thickness of a PDMS membrane can influence its sensitivity. Thinner membranes may exhibit higher sensitivity, and even small deformations can prompt detectable changes in their properties.

4- Fabrication: the practicality of fabricating and handling PDMS membranes can be affected by their thickness. Thick membranes may require longer curing times and more material usage, on the other hand, thick membranes are easier

to deal with while demolding them than thin membranes without taking the risk of being torn.

Figure 5 illustrates the test results for the ultimate tensile strengths of PDMS membranes with different thicknesses. The graph reveals significant variations in both stress and strain across different thicknesses. Thicker membranes (250 μm and 350 μm, as shown in Figure 5) exhibit similar stress-strain curves, characterized by a UTS of approximately 25 Mpa and a fracture strain of around 140%. Conversely, when the thickness of the membrane is reduced to 130 μm, the stress-strain curve diverges significantly from that of thicker membranes (Liu et al. 2009: 2).

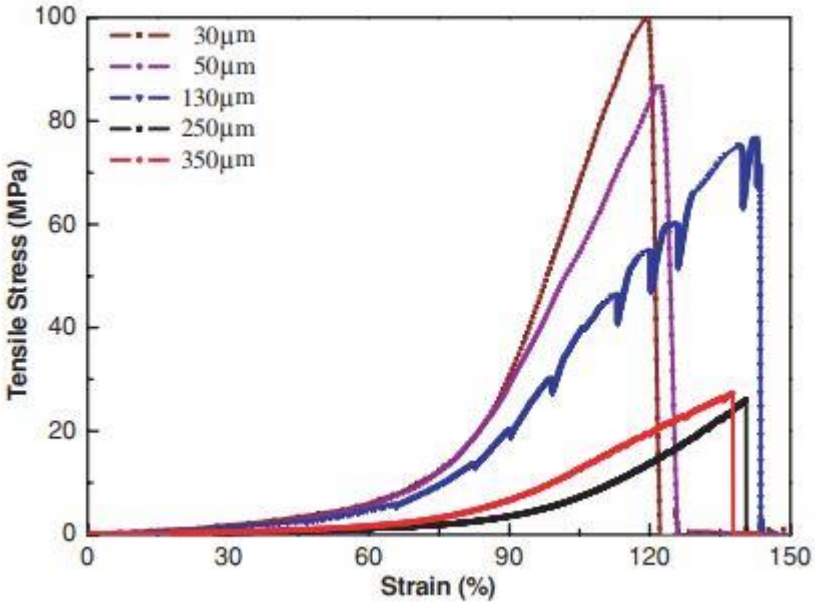

Figure 5: Stress Vs. strain for different membrane thicknesses (Liu et al. 2009: 2).

2.4 STRETCHING METHODS AND DEVICES

Stretching devices that have been developed in past researches usually take into consideration two main aspects which are the engineering and biological factors. Most common techniques used for cell stretching devices are tweezers, micropipettes, and atomic force microscopes but later on, commercial stretching devices step up and took a big place in this market such as Strex systems for cell stretching and Flexcell. Later Flexcell Stage Flexer has been widely used due to its good strain profile, homogeneous strain patterns, and its adaptability for several stretching moods (Kamble et al. 2016: 1).

2.4.1 Actuation Stretching Devices

Several actuation stretching devices are discussed below, and each of them has a different actuation technique.

2.4.1.1 Pneumatic Actuator

The main advantage of a pneumatic actuator is that it's a homogeneous strain actuation that has no direct contact with cells or the surroundings and that prevents contamination. The idea of this stretching device is that the pressure is used to deform the thin membrane and by controlling the pressure the stretching intensity can be controlled (Kamble et al. 2016: 2).

In Figure 6 below Huang and Nguyen developed a pneumatic actuator with vacuum chambers on each side of the membrane, when the chambers are negatively pressured, the membrane will stretch outwards so the cells on the membrane will experience strain (Kamble et al. 2016: 2).

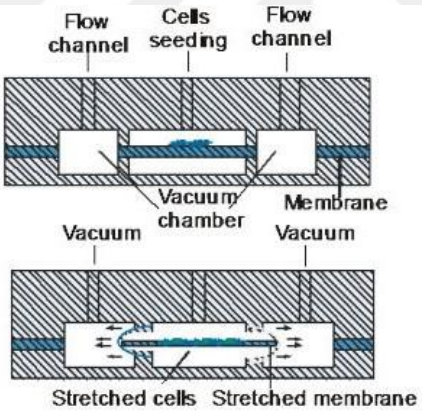

Figure 6: Negative pressure pneumatic stretching device (Kamble et al. 2016: 2).

Another design of pneumatic stretching is shown in Figure 7, this design idea is similar to the previous one but here the stretching occurs radially so the circular membrane is equiaxial stretched. The device consists of a thin PDMS membrane, outer PDMS shell, inner PDMS shell, and rigid glass plate. Firstly, the cells are placed on the membrane Figure 7 (a) then the chambers on the sides are negatively pressured by the connection at the right, the vacuum resulting causes the membrane sides to buckle into the vacuum chambers Figure 7 (b), this causes the membrane to be equiaxial stretched (Kreutzer et al. 2014: 497).

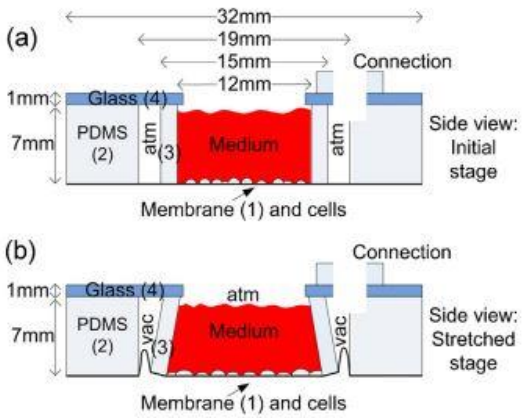

Figure 7: Stretching device mechanism (a) Initial state of the membrane at atmospheric pressure (b) Side chambers are vacuumed causing the membrane to buckle and results in stretching (Kreutzer et al. 2014: 497).

2.4.1.2 Piezoelectric Actuator

The piezoelectric actuator that uses high displacement resolution has been mentioned in several studies, the main advantage of it is that strain values can be precisely controlled but some of them have physical contact with cells and that's an effective downside (Kamble et al. 2016: 3).

Figure 8 below shows the schematic of a piezoelectric actuator with an array of miniature cell stretching chambers that have microwells with a membrane above the piezoelectric pin. The pin is actuated by a piezoelectric actuator using a computer program, this pushes the membrane to give radial strain to every cell (Kamble et al. 2016: 3).

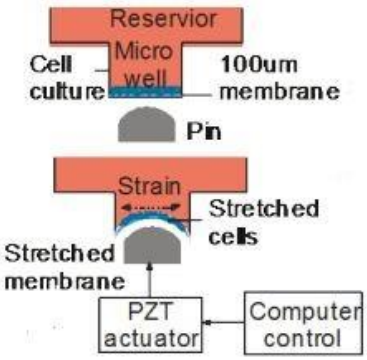

Figure 8: Radial strain pushing pin using a piezoelectric actuator (Kamble et al. 2016: 3).

2.4.1.3 Electromagnetic Actuator

Regarding electromagnetic actuators, despite their high probability for cell contamination because it needs continuous lubrication and possible device erosion,

these kinds of actuators are precise and easy to set up with no complications which makes them widely used. Many custom-made devices are made such as the device designed by Huang, he designed a cell stretching device shown in Figure 9 driven by a servomotor with a fixed membrane holder on a movable plate with an indenter ring at the base that is smaller than the membrane holding ring, the vertical motion downward of the movable plate causes the stretching of the membrane (Kamble et al. 2016: 4).

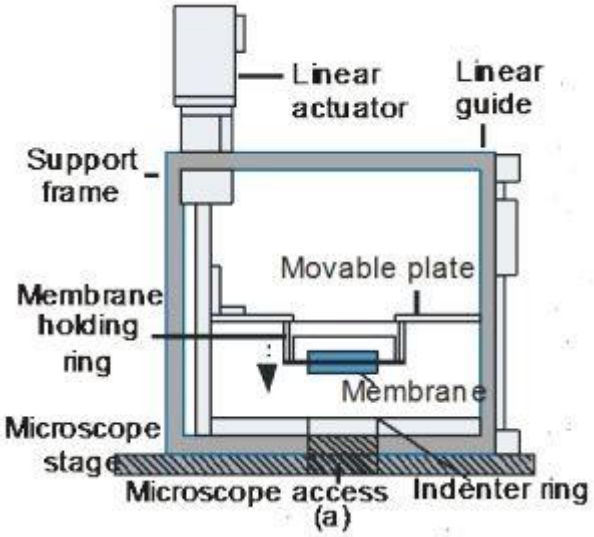

Figure 9: Linear pushing of the movable plate using a servomotor of an electromagnetic actuation device (Kamble et al. 2016: 4).

2.4.2 Stepper Motors Stretching Device

Another type of cell stretching device uses stepper motors with driving belts that cause biaxial motion on the intended membrane. The device shown in Figure 10 consists of two stepper motors each of them is attached to a threaded road, one is responsible for stretching in the x direction and the other is for the y direction. Motors will move the pegs that are connected to the rods, the membrane will be fixed on the pegs so this motion will cause the membrane to experience equibiaxial strain, three of the pegs will be moving and the upper left peg will not (Boynton et al. 2019: 59).

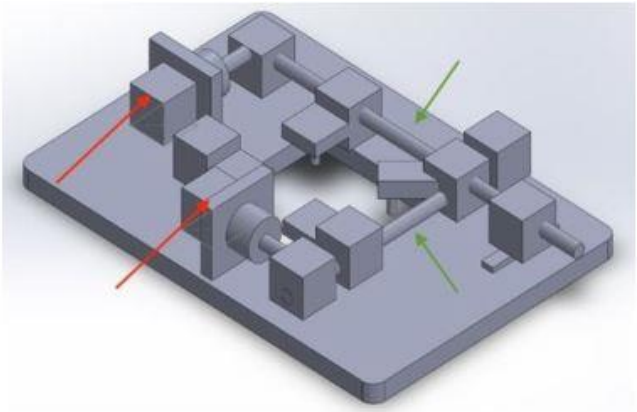

Figure 10: The stretching device with stepper motors is shown by the red arrows and threaded rods are shown by green arrows (Boynton et al. 2019: 60).

2.5 FEA OF PDMS MEMBRANES

Cells on the membrane experience strain when the membrane is being stretched, this strain that's transferred to the cells causes the cells to alter and deform in a specified manner according to the strain intensity. Figure 11 below illustrates how a living cell reacted and changed shape under strain (Boynton et al. 2019: 14).

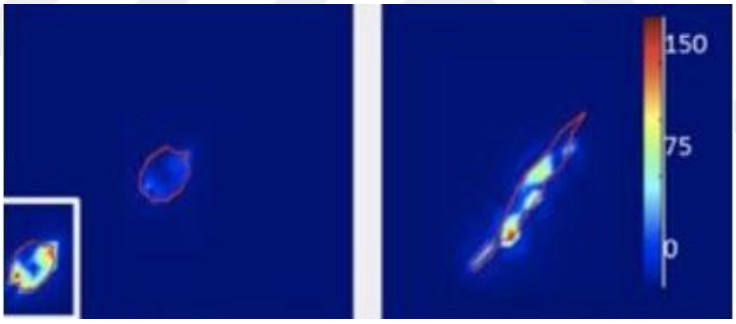

Figure 11: Cell behavior with no strain applied (left) and cell behavior after stretching it on a soft substrate (right) (Boynton et al. 2019: 15).

The first step to analyzing a model is to create the first experimental model of the membrane and test how it will perform then try to improve it until reaching the optimal design. Figure 12 below shows the first design done but when it was tested it showed that it was weak near the corners of the wells so the design is changed accordingly (Boynton et al. 2019: 37).

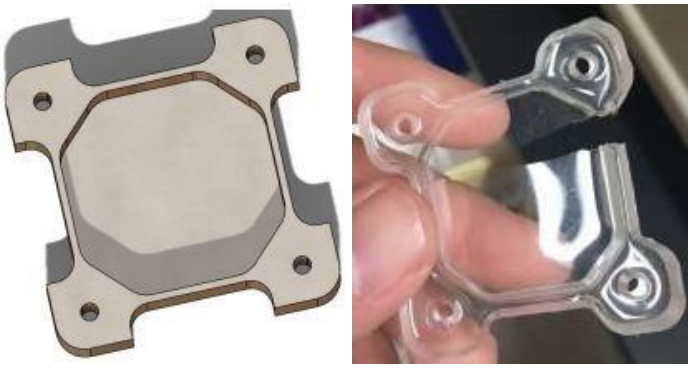

(a) (b)

Figure 12: (a) First design started with (b) Failure of the membrane at the corner of the well (Boynton et al. 2019: 38).

The design later went through several changes as shown in Figure 13, at each stage, the design is modeled on ANSYS by applying force on four holes that make the membrane stretch in a uniaxial way. The main goal of the intended design is to achieve the biggest area possible of uniform strain (Boynton et al. 2019: 40).

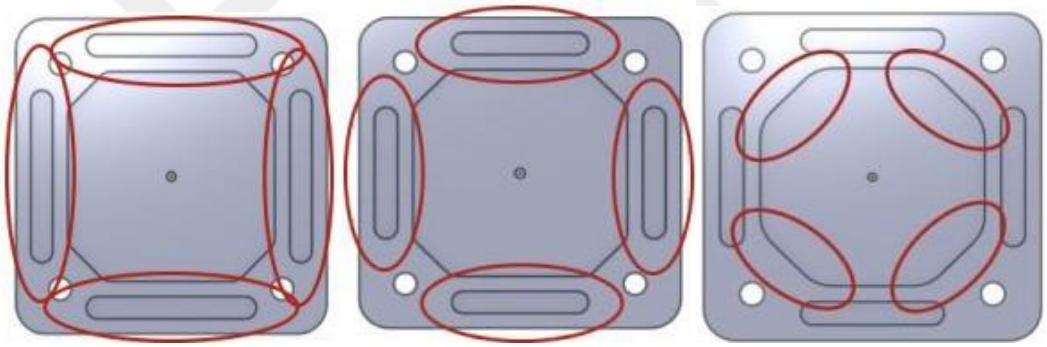

(a) (b) (c)

Figure 13: Three membrane prototypes each of them with a different design, changes done are denoted by red ovals. (a) Design 1 with sharp corners and long wells (b) In design 2 the wells are shortened (c) In design 3 the edges are elongated and the corners are curvy (Boynton et al. 2019: 40).

In Figure 14 each of the three designs mentioned earlier is modeled using ANSYS software, the modeling showed the uniform strain area of each membrane by percentage of the total area of the membrane. The results showed how design two gave the largest area so it's been determined as the optimal design, later on, the mold is produced for membrane production (Boynton et al. 2019: 41).

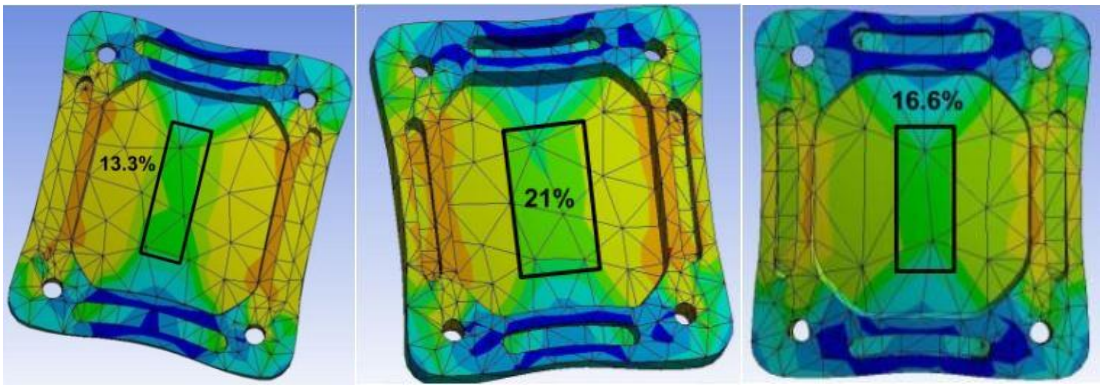

(a) (b) (c)

Figure 14: (a) Design 1 with a uniform strain area of 13.3% of the membrane (b) Design 2 with a uniform strain area of 21% of the membrane (c) Design 3 with a uniform strain area of 16.6% of the membrane (Boynton et al. 2019: 41).

Another important aspect that has been discussed is the effectiveness of the membrane size on stretch uniformity. Figure 15 shows three sizes of PDMS membranes, 40mm×40mm, 40mm×20mm, and 40mm×14mm. The result of the FE simulation of the logarithmic tensile strain field throughout the membrane showed that even though the strain field pattern differs between the three sizes but the center part of the membrane where the cells will be cultured went uniform for all of them. Note that the membranes are fixed on the left edge and while the right edge is displaced by 15% and the membrane thickness of 200 μm (Shao et al. 2013: 4).

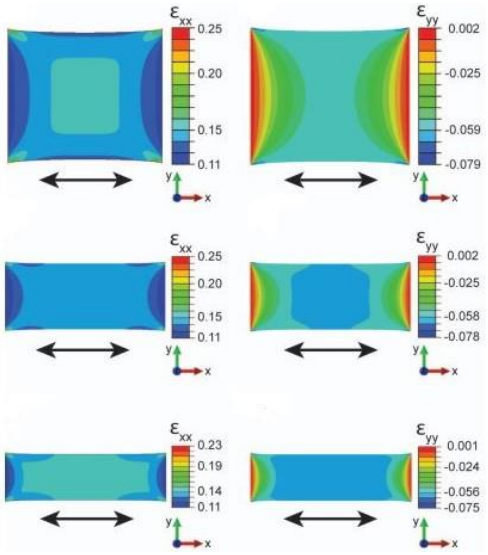

Figure 15: On the left side is the tensile strain fields εxx and on the right side is the tensile strain field εyy (Shao et al. 2013: 4).

2.6 EFFECT OF PDMS TO HARDENER RATIO

The important thing to consider during the manufacturing process of the PDMS membrane is the PDMS to hardener ratio, the ratio effects directly the elastic

modulus and tensile strength of the membrane when it undergoes mechanical tests (Izdihar et al. 2021: 1). By increasing the hardener, the membrane will become stiffer and stronger but it will lose elasticity, elasticity is needed in cell cultivating to observe the cells behavior when the strain is transferred from the membrane to the cells, so the more elastic the membrane more strain can be monitored on the cells. With that being said it's important to reach a mixture ratio that makes it strong and withstand tearing but at the same time elastic enough.

In a previous study, this subject was discussed and tested, two polymer-based materials, polydimethylsiloxane (PDMS) and silicone elastomer (SE) are used to produce several membranes with different ratios and thicknesses. Firstly, for PDMS, the mixture is hand stirred for around 5 minutes then a vacuum pump is used to remove all of the air bubbles within the mixture to make sure it's clean and equally dense, after that the samples were cured in the oven for 30 minutes at 80 °C then the temperature is increased to 100 °C for one more hour. Lastly, the cured samples were left to cool down to room temperature. For silicon elastomer, the mixture is cured at room temperature (23 °C), but both materials were cast on a petri dish which makes it easier in removing the membrane. Table 1 below shows the samples produced (Izdihar et al. 2021: 4).

Table 1: Samples with different mixtures of (SE) and (PDMS) (Izdihar et al. 2021: 4).

	PDMS		**SE**	
Thickness, Weight / **Sample No.**	Thin, 11 g	Thick, 22 g	Thin, 22 g	Thick, 22 g
1	PDMS 9.5/1.5	PDMS 19/3	SE 4.5/5.5	SE 10/12
2	PDMS 10/1	PDMS 20/2	SE 5/5	SE 11/11
3	PDMS 10.5/0.5	PDMS 21/1	SE 5.5/4.5	SE 12/10

Samples were cut into a specimen shape and a tensile test is done for them to test their strength, they were pulled by a force of less than 15 N. The tensile test for the PDMS samples showed that the tensile strength increases by increasing the crosslinker however further increasing of the crosslinker decreases the tensile strength by reducing the curing agent. Also, it's been shown that lighter samples are stiffer than heavier ones. As shown in Figure 16 bellow, PDMS showed better results in terms of

tensile strength than SE which gives a higher advantage for PDMS for using it in medical approaches (Izdihar et al. 2021: 7).

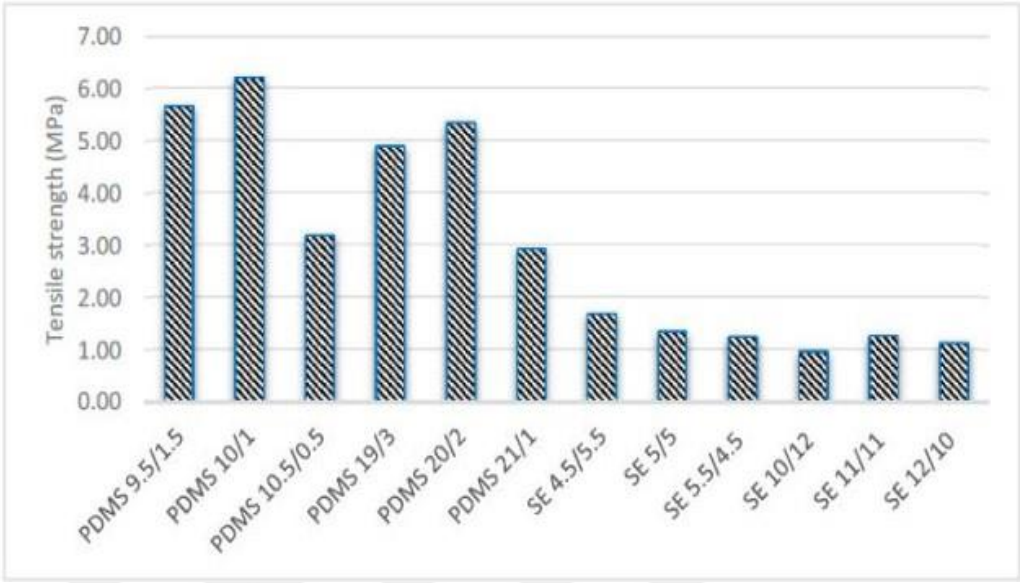

Figure 16: Tensile strengths for PDMS and SE with various mixtures and thicknesses (Izdihar et al. 2021: 7).

It's shown in Figure 17 the effectiveness of mixing ratio on the elastic modulus at a crosshead speed of 5mm/min, as the ratio increases elastic modulus increases until the ratio reaches 9:1, after that increasing the ratio will decrease the elastic modulus proved by 10:1 ratio, this is linked to the fact that increasing the crosslinker slows the curing rate of PDMS, thus, the higher the base in the mixture the more unreacted base polymer are and softer the material at the end (Khanafer et al. 2009: 505).

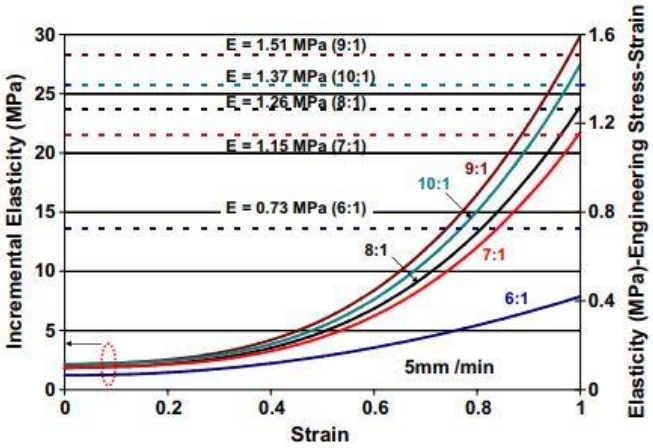

Figure 17: Effectiveness of mixing ratio on the elastic modulus at 5mm/min crosshead speed (Khanafer et al. 2009: 505).

CHAPTER III

RESEARCH METHODOLOGY AND METHOD

3.1 INTRODUCTION

This study aims to model the behavior of a polydimethylsiloxane membrane when the membrane is subjected to a strain percentage by using a finite element analysis approach. These membranes are used in medical applications to mimic human tissues and how tissues will react under deformation, so it's important in this research to take into consideration all the factors that may affect the membrane behavior.

Membranes produced with different designs and experimental conditions during the study were sent to the electrical department of Hacettepe University to test them with a stretching device to examine their durability and failure under different strain percentages and stretching speeds. This chapter is conducted as followed:

1- Membrane Design Using FEA
2- Membrane Fabrication and Apparatus
3- Stretching Device and Tearing
4- FEA of the Membrane

3.2 MEMBRANE DESIGN USING FEA

The membrane design went through a lot of enhancements to reach the optimal design. The important thing to consider while designing the membrane is that when it's under strain, the strain uniformity through the used membrane area should not exceed 20 % due to medical application reasons, with that being said several membrane designs were put
into analyzing through the FEA software (ANSYS) to see which of these designs gives the largest usable area.

When designing a new membrane, we aim to achieve a uniform strain distribution, high durability, and cost-effectiveness while maximizing the cell culture

area. In pursuit of these goals, we have proposed and analyzed several geometric designs, including a square chamber with chamfered edges, a square chamber with

fillet edges, and circular chamber membrane designs, as depicted in Figure 18. The shape of the membrane will directly contribute to the outcome and selection because the strain is transferred through the membrane and the shape of the membrane will determine how it will travel through.

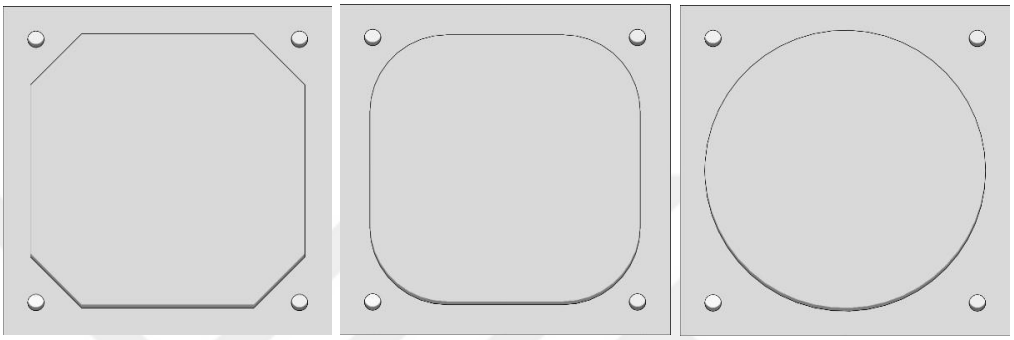

(a) (b) (c)

Figure 18: Membranes with (a) Square chamber with chamfered edges, (b) Square chamber with fillet edges, (c) Circular chamber.

For the three membranes, the strain distribution has been calculated in Figure 20. The loading is applied by fixing one corner and pulling from the other three corners, as shown in Figure 19.

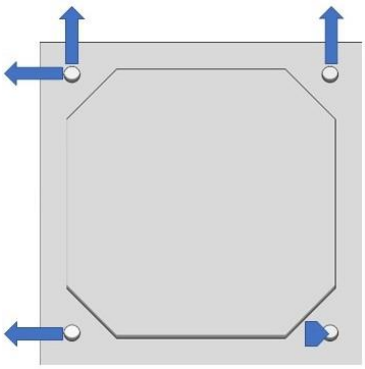

Figure 19: Membrane Stretching on X and Y axis with the bottom right hole fixed.

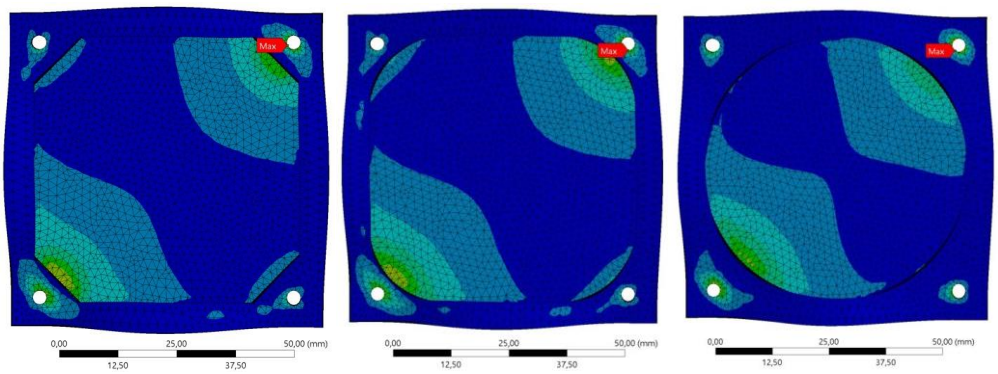

Figure 20: Strain distribution in the membranes of different geometries.

Using the results of strain distribution, we defined a parameter called the uniformity index to evaluate the performance of the membranes. The uniformity index is calculated using equation 3.1 as follows

$$\text{Uniformity index} = \frac{\text{Uniform area}}{\text{Total area of membrane}} \tag{3.1}$$

$$\text{Chamfered edge membrane } \frac{1327\ mm^2}{2650\ mm^2} = 0.5$$

$$\text{Rounded edge membrane } \frac{1275\ mm^2}{2650\ mm^2} = 0.48$$

$$\text{Rounded membrane } \frac{845\ mm^2}{2123\ mm^2} = 0.4$$

The uniformity index for membrane with a square chamber and chamfered corners, square chamber and rounded corners, and the circular chamber is calculated as 0.5, 0.48, and 0.40, respectively. It is worth mentioning that the circular chamber has a smaller area than the others, meaning that the number of cells that can be cultured is low. It can be seen in Figure 20 that under these loading conditions, the strain is uniform only at the central portion of the membrane. Therefore, we have decided to change the loading. Instead of pulling the membrane from the corners, we tried to pull it from the side edges,by removing the holes from the edges and reorienting them on the sides. The design with 4 holes at the edges is changed because of the mechanism of the stretching device, it will stretch the membrane from the side edges not from the edges, as shown in Figure 21, to keep the force vectors on X and Y without components, this is regarded to the complication in design and manufacturing of the device that comes if 4 more motors are added to the edges. More holes are added to avoid large differences in stress and strain in different membrane areas. The final design of the membrane is shown in Figure 22.

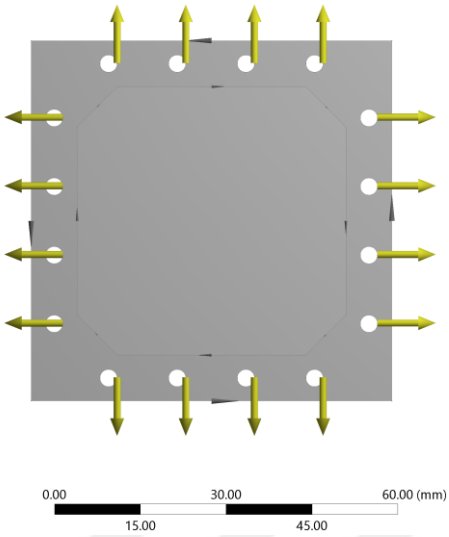

Figure 21: Final membrane design with displacement applied on X and Y axis.

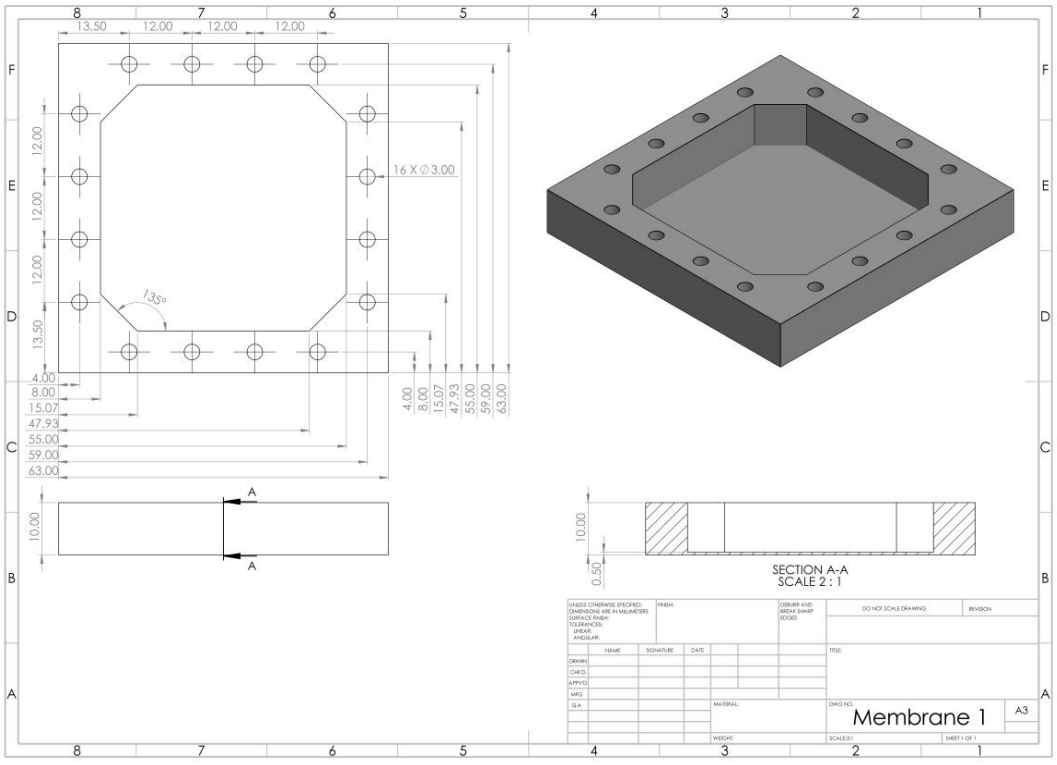

Figure 22: The geometry and dimensions of the optimized membrane.

3.3 MEMBRANE FABRICATION AND APPARATUS

3.3.1 Polydimethylsiloxane

Polydimethylsiloxane is a hyperelastic material which means that when it's subjected to strain it expands in the area in a hyperelastic manner and it goes back to its original dimensions when strain is back to zero, the ability of hyperelastic materials to withstand high strain rates with low stress is much higher than elastic materials as

shown in Figure 23 (Phothiphatcha and Puttapitukporn 2021: 13). And since the material is hyperelastic, by changing the membrane design, curing time, cross-linker, or hardener to polydimethylsiloxane ratio mixture, all of these factors have a direct effect on the membrane behavior when its set to test.

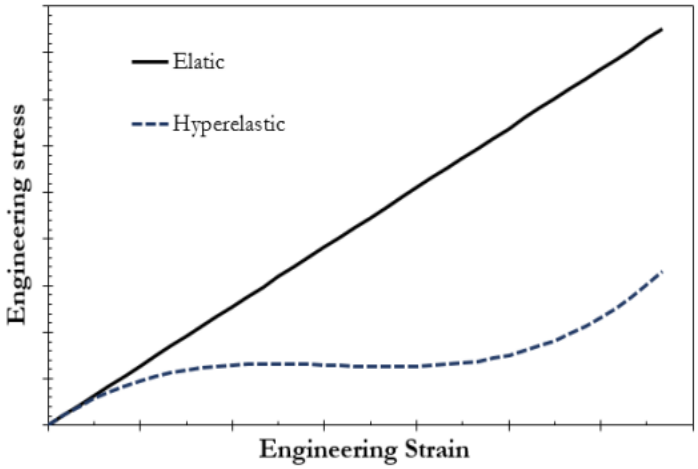

Figure 23: Stress-strain graph showing the difference between elatic and hyperelastic materials (Phothiphatcha and Puttapitukporn 2021: 13).

3.3.2 Mold

After choosing the membrane design that will be tested depending on several variables as mentioned earlier the mold is set for design, the mold design serves several needs, first of all, the mold is designed for higher membrane production rates, it has four slots each of them is an individual membrane chamber, secondly, it should be handy for removing the membrane from the mold after its cured and cooled down without the risk of being torn especially because the membrane is really thin, accordingly the mold is being designed in a way that when it's time for removing, the whole upper cover of the mold will be dismantled by unscrewing the screws as shown in Figure 24, also the inner sides of the cover and the sides of the membrane core are drafted outwards by 3 degrees that will help also is membrane removal.

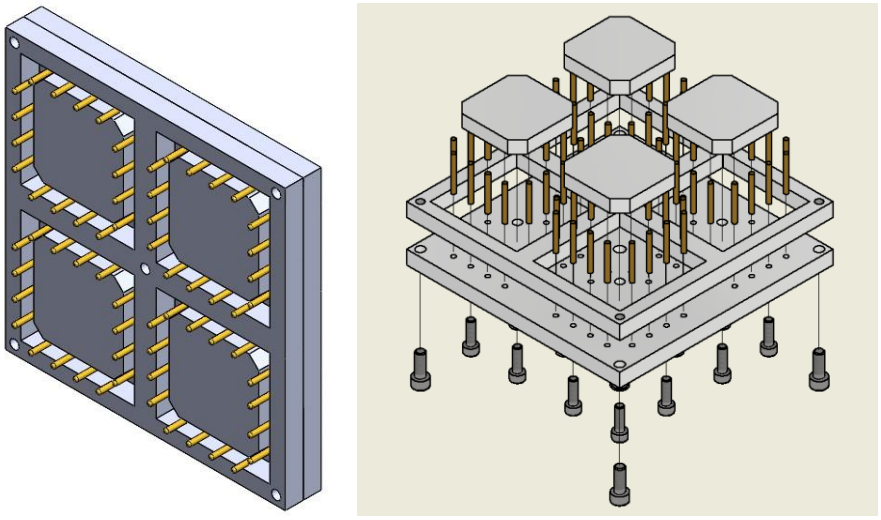

(a) (b)

Figure 24: (a) Isometric CAD view of the mold (b) Exploded CAD view of the mold showing each component.

It's taken into consideration that the mold also should fit the vacuum chamber and the oven in order not to face any problems due to its size. Also, the middle part of each mold slot is detachable for cleaning purposes and is ground by using sandpaper and then polished with fine Al_2O_3 to make sure that the membrane will be fine and free of scratches as shown in Figure 25 (a). Later on, the mold experienced leakage of PDMS between the mold body and the cover, a water leakage test is done and it showed the leakage points and the solution was by adding two screws to each of the four sides as shown in Figure 25 (b), the water test is done again which didn't show any more leakage.

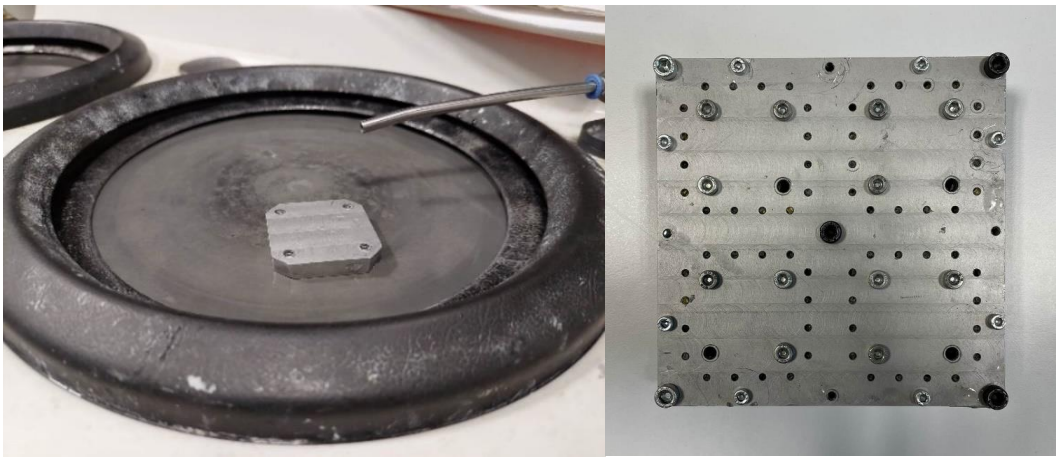

(a) (b)

Figure 25: (a) Membrane core sandpapered (b) Mold after adding two screws to each side to avoid PDMS leakage.

To select the proper material model for our study, tensile test specimens are fabricated according to ISO527-2-5A standard. The solid model of the specimen can be seen in Figure 26 (a). The mold for the specimen has been manufactured from brass by CNC machining and is shown in Figure 26 (b). The specimen produced by casting is shown in Figure 26 (c).

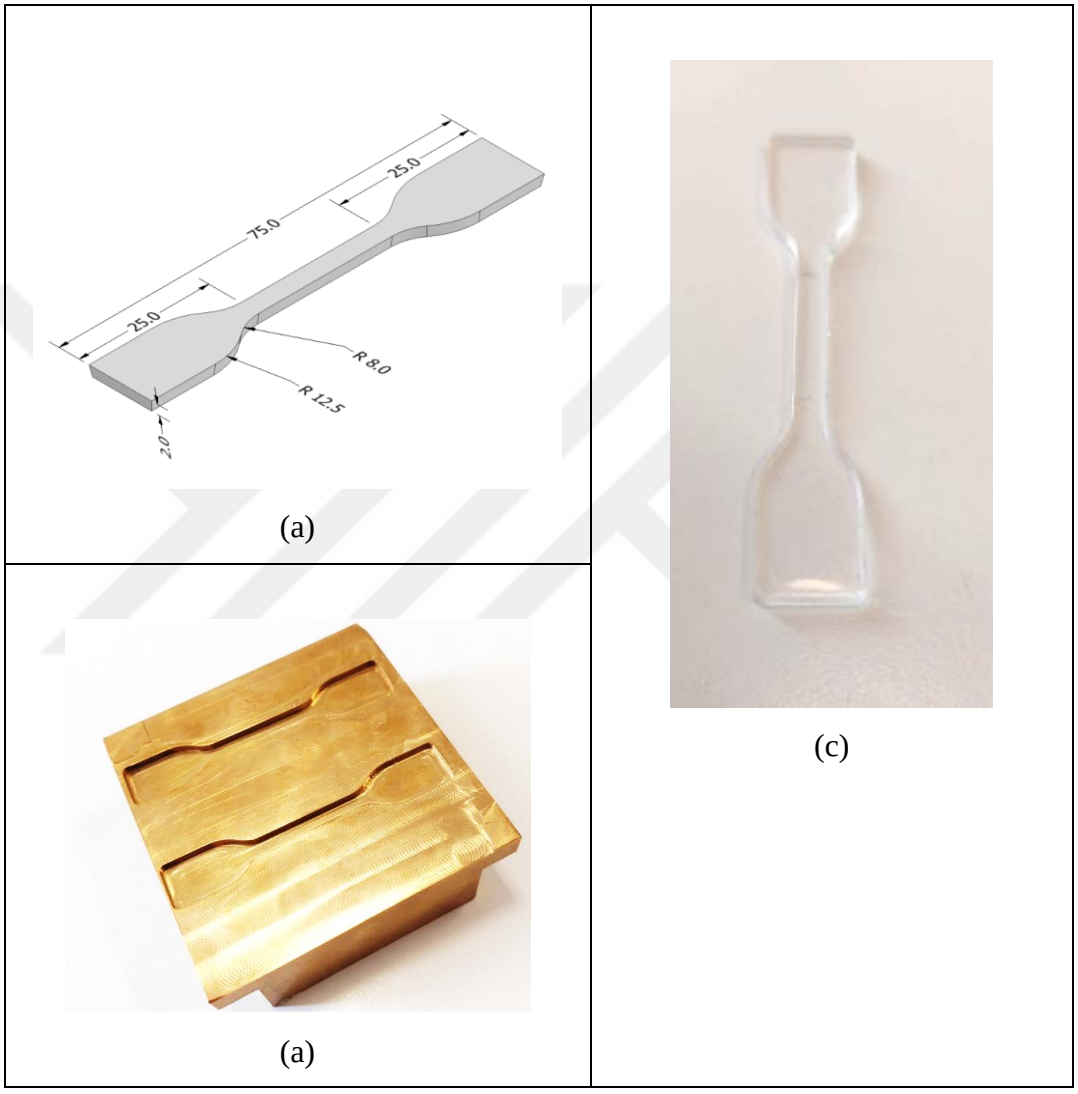

Figure 26: (a) The solid model of the tensile test specimen, (b) The mold used for casting the PDMS specimen, (c) de-molded PDMS tensile specimen.

3.3.3 Apparatus

The three main apparatuses used were 1-Weighing Balance 2-Vacumm Chamber 3-Oven. There are some other parts like the hammer, screwdriver, and detaching rod (used for detaching membrane from the mold after being cured).

Weighing Balance Figure 27 (a) is used to measure the weight of the PDMS and hardener (in grams) that will be mixed in a specific ratio, also knowing the exact

weight needed from each of them prevents wasting material because mixing them will either used or thrown away and they cannot be separated.

Vacuum chamber Figure 27 (b) is used after pouring the mixture into the membrane, its job is to remove all air bubbles and impurities within the mixture, this process is done several times until no more bubbles emerge from the mixture.

(a) (b)

Figure 27: (a) Weighing balance (b) Vacuum chamber.

When the mixture is ready to be cured its placed in the oven Figure 28 (a) with the temperature and time needed for curing the PDMS. The oven is balanced using a water gauge Figure 28 (b) to make sure there is no tilt, balancing the oven is essential to make sure that the membrane is having the same dimensions from all sides so the mixture won't swivel around and stay evenly distributed, not thick on a side and thin on the other.

(a) (b)

Figure 28: (a) Mold in oven (b) Balancing oven using water gauge.

3.3.4 Membrane Manufacturing

The membrane production process contains several steps. First of all, the PDMS is mixed with the hardener in a specific ratio of 0.5:10, 0.75:10, or 1:10 in grams, here the hardener which can be called also the crosslinking agent increases the cross-linking structure of the material which is a result raises the hardness of the membrane but also reduces its elasticity. After the mixture is well mixed and homogeneous Figure 29 the mixture is poured into the mold to take the shape Figure 30 (a), then the mold is placed into the vacuum chamber Figure 30 (b) to make sure all the air bubbles and impurities are extracted, this process is repeated several times until the mixture stops air bubbles emerging. Then the mold is taken to the furnace so the mixture is cured, the curing parameters which are the furnace temperature and time are (60°C, 4 hours) or (80°C 30 minutes then 100°C 1 hour) respectively.

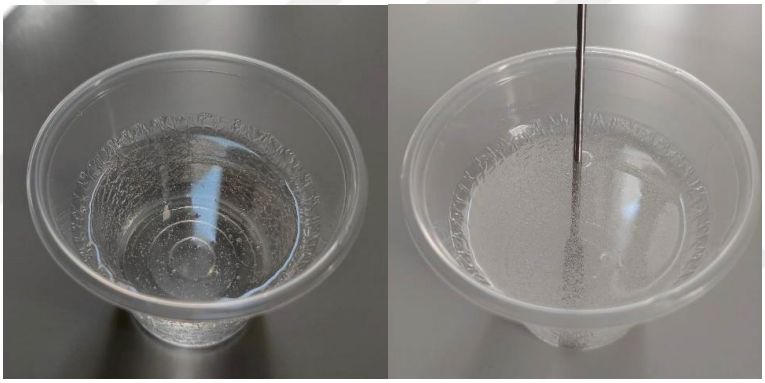

(a) (b)

Figure 29: (a) PDMS and hardener before mixing (b) PDMS and hardener after mixing and being homogeneous.

(a) (b)

Figure 30: (a) Mold after pouring the mixture (b) Mold in the vacuum while air bubbles are extracted.

Then the mold is taken out from the oven and set to cool down and after that the mold and pins are dismantled and the membrane is taken out carefully to avoid

tearing as shown in Figure 31 (a). The mold and pins are later submerged in acetone Figure 31 (b) to clean them before manufacturing again.

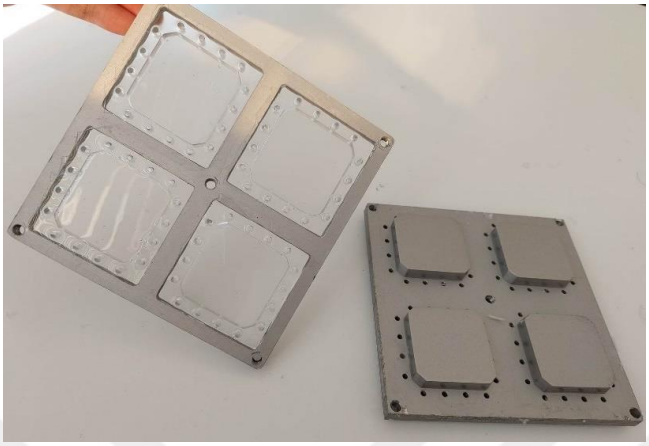

(a)

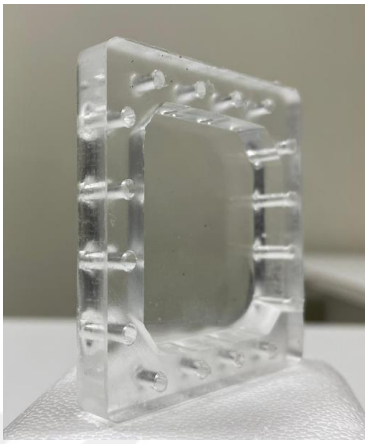

(b)

(c)

Figure 31: (a) Membrane demolding (b) Fabricated PDMS membrane (c) Mold and pins submerged in acetone after demolding for cleaning.

3.4 STRETCHING DEVICE AND TEARING

3.4.1 Stretching Device

The biaxial stretching device used for testing the membrane was designed and manufactured by Hacettepe University, shown in Figure 32.

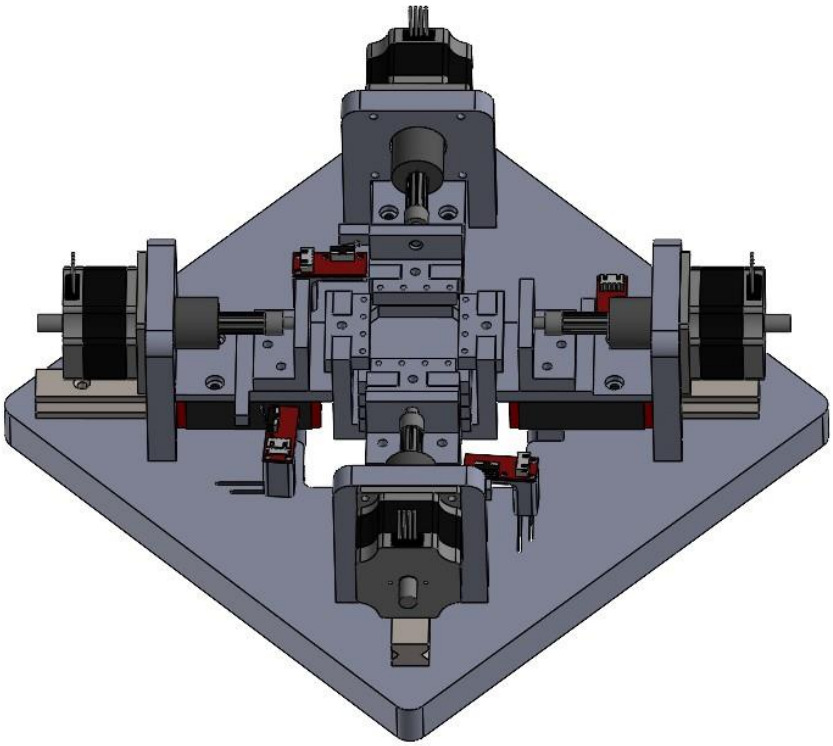

Figure 32: Stretching device (Isometric view).

3.4.2 Tearing

After an optimized size and geometry have been decided by finite element analysis in terms of stress levels, still some failures due to the tearing have been observed during biaxial stretching. To further improve the membrane performance PDMS fabrication conditions have been changed. It is worth mentioning that the ratios are determined by pilot experiments. For hardener ratios more than 1:10, the membrane becomes too stiff to be stretched, and for ratios less than 0.5:10, it cannot withstand the applied loads.

When the ratio of the hardener to the PDMS matrix has been changed. When the amount of hardener decreases, the elasticity modulus also decreases, which means that the membranes gain more flexibility but their durability is lower. Another control factor is the curing time and temperature that need to be optimized. For this, various combinations have been tried and the membrane has been subjected to biaxial tests as shown in Figure 33. The medical department of Hacettepe University concluded that a membrane that can withstand more than six continuous hours of sinusoidal tension would be fit for their tests.

Table 2: Different testing conditions for membranes and results, (✓, pass) (X, fail).

Hardener: PDMS ratio	**Four hours at 60°C**			**30 minutes at 80°C + 60 minutes at 100°C.**		
	Strain (%)			Strain (%)		
	10	**15**	**20**	**10**	**15**	**20**
1:10	X	X	X	X	X	X
0.75:10	✓	✓	✓	✓	✓	✓
0.5:10	✓	X	X	✓	X	X

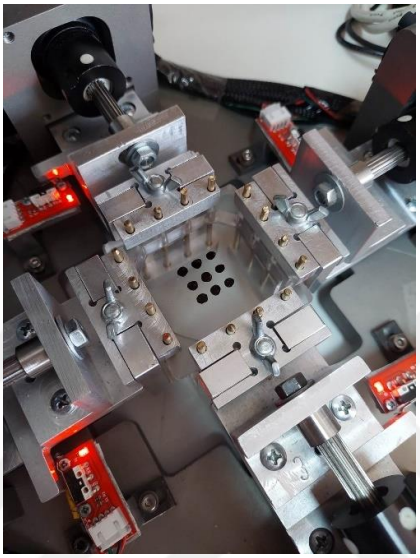

Figure 33: Membrane installed on the stretching device and tested.

Table 2 gives an overview of the membranes manufactured and which gave the best result. The important thing to note is that any of the failing membranes above have failed to withstand 10%, 15%, or 20% displacement for 6 continuous hours that doesn't mean that all failed at the same point, some are torn after a short time and others stood more. Also, the testing team at Hacettepe tested the membranes at different lap speeds so they had a couple more factors that gave the result that the membrane with a ratio of 0.75:10 grams (hardener to PDMS) is the optimal membrane. Tearing usually occurred from the edges that connected the membrane body to the thin membrane area and specifically from the pin holes as shown in Figure 34.

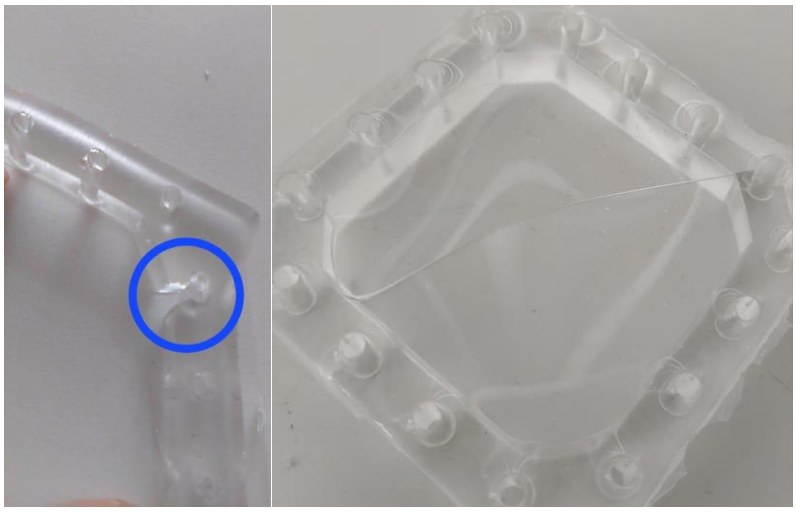

(a) (b)

Figure 34: (a) Tearing occurred from the pin holes (b) Full membrane tearing.

3.5 FEA OF THE MEMBRANE

3.5.1 Background

In modeling materials, there are several methods and each of these methods may be suitable for one case and not suitable for the other, this depends on factors such as the material properties and the parameters in which the case is tested. In the case of elastic materials properties are determined by the function U which is the strain energy per volumes unit for a given material, while in this case which is concerned about modeling a hyperelastic material is based on the strain energy function U that can be treated as a function based on strain potential strain function (Elgström 2014: 22).

3.5.2 Different Modeling Methods

In hyperelastic materials there are several methods to model their nonlinear stress-strain behavior, three methods are discussed as followed.

3.5.2.1 Ogden Model

This is one of the most widely used models for hyperelastic materials even more than the polynomial method because it's more computationally intensive. Ogden model proposes the strain energy function based on the principal stretches (λ1, λ2, λ3) for incompressible materials that are assumed λ1λ2λ3=1 (Ali et al., 2010). This model was developed by Raymond Ogden in 1972 and the equation 3.2 was obtained

$$U = \Sigma_{i-1}^{N} \frac{2\mu_i}{\alpha_i^2}\left(\bar{\lambda}_1^{\alpha_i} + \bar{\lambda}_2^{\alpha_i} + \bar{\lambda}_3^{\alpha_i} - 3\right) + \Sigma_{i=1}^{N} \frac{1}{D_i}(J_{el} - 1)^{2i} \qquad (3.2)$$

Where:

$\bar{\lambda}_i = J^{\frac{-1}{3}}\lambda_i$

$J = \lambda_1\lambda_2\lambda_3$

λ_i = The principal stretches

J = The Jacobian determinant

J_{el} = The elastic volume ratio

D_i = Material constant, introduces compressibility and is set equal to zero for fully incompressible materials

The constants μi and αi describe the shear behavior of the material.

3.5.2.2 Mooney-Rivlin Model

In the 1950's Mooney and Rivlin proposed the nonlinear elasticity theory, the strain energy potential equation 3.3 as mentioned earlier is (Ali et al. 2010: 234)

$$U = \Sigma_{i,j=0}^{N} C_{ij}(\bar{I}_1 - 3)^i(\bar{I}_2 - 3)^j + \Sigma_{i=1}^{N}\frac{1}{D_i}(J_{el} - 1)^{2i} \quad (3.3)$$

Where:

C_{ij} = The material parameter

$C_{00} = 0$

So, the first order of the equation is as followes

$$U = C_{10}(\bar{I}_1 - 3) + C_{01}(\bar{I}_2 - 3) \quad (3.4)$$

Setting N=0 and $\alpha_2 = -2$ in Ogden model, Mooney-Rivlin equation is obtained as

$$U = \frac{\mu_1}{2}\left(\bar{\lambda}_1^2 + \bar{\lambda}_2^2 + \bar{\lambda}_3^2 - 3\right) - \frac{\mu_2}{2}\left(\bar{\lambda}_1^{-2} + \bar{\lambda}_2^{-2} + \bar{\lambda}_3^{-2} - 3\right) \quad (3.5)$$

Where

$C_{10} = \frac{\mu_1}{2}$, $C_{01} = -\frac{\mu_2}{2}$

There are different orders of the Mooney-Rivlin equation and as the order gets higher the results will be more accurate, higher order means a more accurate stress-strain curve will be approximated, but the downside of it is that by increasing the order

it will be harder for the software to give results and that makes it important to pick the suitable equation order modeling. By setting N=2 in equation 3.3 will give fifth order Mooney-Rivlin and by setting N=3 we will obtain ninth order Mooney-Rivlin. Calculating higher-order equation is not feasible that's why advanced modeling program like ANSYS is used to calculate and give the stress-strain curve approximation.

The favorite for material modeling are Ogden and Mooney-Rivlin models, by the major downside for them is that the parameters should be obtained by experiments so they are not physically based parameters (Ali et al. 2010: 234).

3.5.2.3 Yeoh Model

When N=3 in the reduced polynomial model, the strain energy function equation 3.6 of the Yeoh model is as followes

$$U = \Sigma_{i=1}^{3} C_{i0} (\bar{I}_1 - 3)^i + \Sigma_{i=1}^{3} \frac{1}{D_i} (J_{el} - 1)^{2i} \tag{3.6}$$

Were the bulk modulus equation 3.7 and the shear modulus equation 3.8 are

$$K_0 = \frac{2}{D_1} \tag{3.7}$$

$$\mu_0 = 2C_{10} \tag{3.8}$$

Yeoh model is applicable for a wider range of deformation and its able to predict the stress strain behavior from data gained from one deformation mode such as uniaxial extension (Ali et al. 2010: 235). This model is used for incompressible and nonlinear elastic materials like rubbers (Phothiphatcha and Puttapitukporn 2021: 14).

3.5.3 Ansys Modeling

After presenting the most efficient and widely used methods of hyperplastic material models, each of these three material models mentioned earlier is used on the selected membrane to test it. In general, the modeling is done under the same conditions. The ratio of PDMS to hardener and the modeling method are the two factors that change from one model to the other.

3.5.3.1 PDMS To Hardener Ratio

The first factor that can change from one model to another is the PDMS to hardener ratio, the ratio difference plays a role in how the membrane will react when its stretched, by increasing the hardener the membrane will gain more strength but on the other hand it will lose some of its elasticity and vice versa for the PDMS.

To be able to simulate different ratios, stress-strain values should be imported to each model, these values represent the stress-strain the membrane undergoes under tension for each ratio. The tensile test and numerical simulation of PDMS with different ratios are taken from Figure 35 (Chang et al. 2020: 7436), then by using the Web Plot Digitizer tool the values are extracted from Figure 36 and ready to be imported to Ansys. All stress-strain values for each ratio are shown in Appendix A table 6.

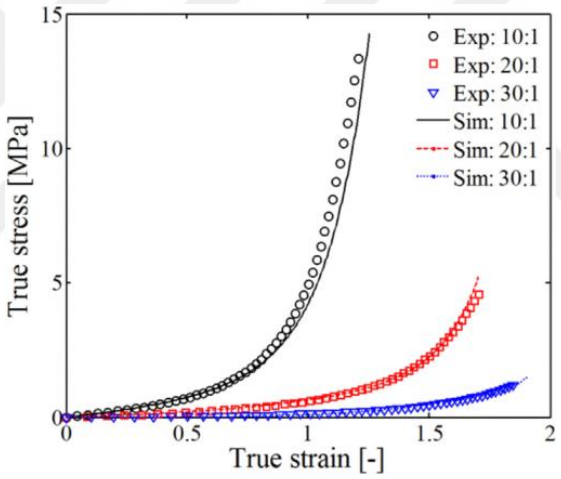

Figure 35: Experimental and simulated stress-strain values of different PDMS to hardener ratios for a uniaxial tension test (Chang et al. 2020: 7436).

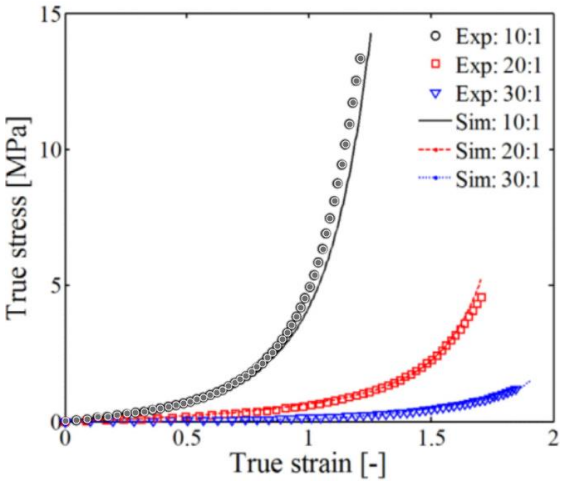

Figure 36: Grey dots are assigned in place on the graph to get the stress-strain values, this is done to each of the three different ratios using Web Plot Digitizer.

3.5.3.2 Modeling Procedure

Ansys use a finite element approach to analyze models, this is a method for numerically solving differential equations. Ansys have several analysis systems for many fields such as thermal, fluid flow, electrical, rigid dynamics and many others. The one that's used in this modeling is static structural analysis system because it meets the needs of analyzing strain and stress of the membrane.

The incompressibility parameter D1 is calculated by the following equation 3.9

$$D1 = \frac{2}{k} \tag{3.9}$$

Where:

k= Bulk modulus

Bulk modulus is given by the following equation

$$k = \frac{E}{3(1-2v)} \tag{3.10}$$

Where:

E= Elastic modulus

v= Poisson's ratio

The elastic modulus of the PDMS ranges from 0.57 MPa to 3.7 MPa (Wang et al. 2014: 1). The elastic modulus represents the ability of the material to be deformed by stretching and going back to its original shape or not, low elastic modulus means that the material is rubberlike material and can be easily stretched and high elastic modulus is the opposite (Ashby and Jones 2012: 116). By increasing the crosslinker to the PDMS this makes it less elastic and stiffer, so elastic modulus should be higher for the mixture with more hardener in it and lower for the mixture with less hardener. With that being said elastic modulus for the three ratios in table 3 is assumed accordingly as followed

Table 3: Hardener/PDMS ratio and assumed elastic modulus.

PDMS/Hardener (in grams)	Elastic Modulus (MPa)
1:10	3.7
0.75:10	2.1
0.5:10	0.57

Regarding PDMS Poisson's ratio its exact value is not known but it ranges between 0.45 and 0.5 (Cho et al. 2021: 5), and its assumed here to be 0.47. Now for calculating incompressibility parameter for 1:10 hardener to PDMS mixture use equation 3.10 to find bulk modulus

$$k = \frac{3.7\ \text{MPa}}{3\left(1 - 2(0.47)\right)}$$

$$k \approx 20.6$$

Then use equation 3.9 to find the incompressibility parameter

$$D1 = \frac{2}{20.6}$$

$$D1 \approx 0.1$$

Table 4 bellow shows the incompressibility parameter for each ratio.

Table 4: Incompressibility parameter for each ratio.

Hardener/PDMS (in grams)	Incompressibility parameter (D1)
1:10	0.1
0.75:10	0.2
0.5:10	0.6

Quarter membrane is imported to Ansys since symmetry will be used, faces of symmetry is assigned in Figure 37 (a), then a displacement of 10% which is 3 mm is applied on the holes Figure 37 (b).

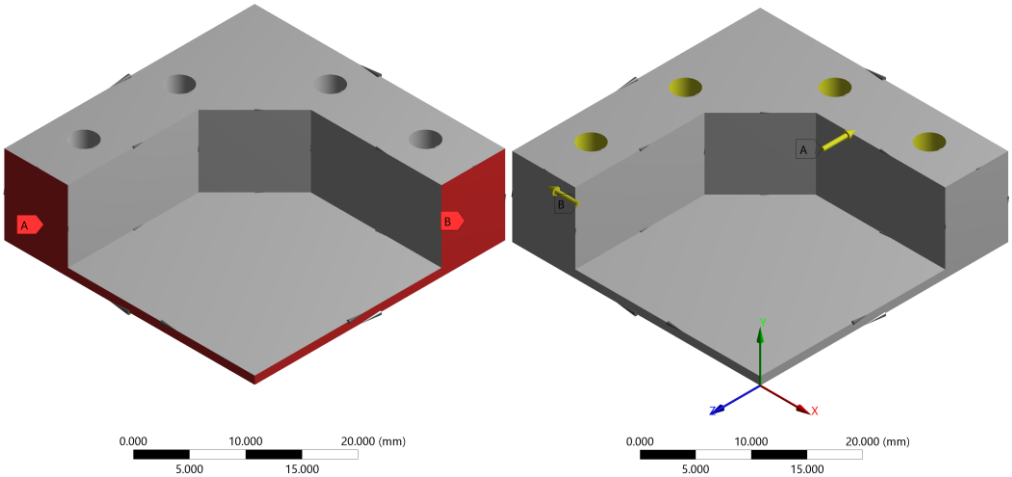

(a) (b)

Figure 37: (a) Symmetry assigned on faces A and B for the membrane (b) Displacement applied on holes.

A path is defined on the membrane to see how the strain and stresses are behaving through the membrane. The path starts from the middle edge of the membrane (point 1) and ends at the middle (point 2) shown in Figure 38, since symmetry is used for solving, the rest of the 3 quarters will give the same stress and strain values as this quarter gives. The stress and strain values are then graphed and shown in Chapter 4.

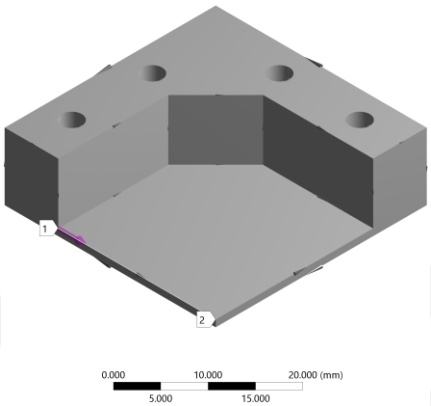

Figure 38: The path assigned to give the strain and stress behavior under the assigned displacement.

Similarly, a PDMS specimen is modeled using the three material models. Symmetry is also used to model the specimen; displacement is applied to the specimen to compare each model with the real experimental specimen that has been tensile tested in the lab of METU. The aim of this is to know which of the three material models is the most accurate. Faces of symmetry are assigned in Figure 39 (a), then the displacement is applied in Figure 39 (b).

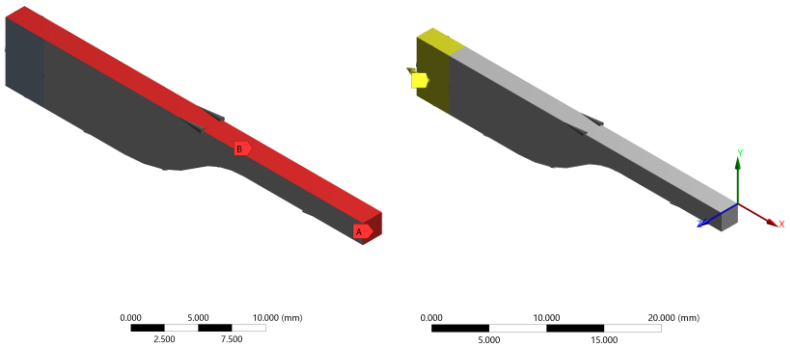

(a) (b)

Figure 39: (a) Symmetry assigned on faces A and B for the specimen (b) Displacement is applied in the specimen.

The specimens which were sent to METU to be tested came out with different results due to the variations in production in terms of PDMS to hardener ratio and/or curing time and temperature in the oven. To find out the best material model, all three material models mentioned earlier are compared to a real specimen tested which ratio is 1:10, and the curing time is 4 hours at 60 °C, which specimen is picked doesn't matter in this case as long as the uniaxial test data picked for specimen modeling is corresponding to the PDMS to hardener ratio of the real specimen. The aim is to find which of the material models gives the closest values to the experimental specimen, Figure 40 below shows the extension vs load for the experimental specimen.

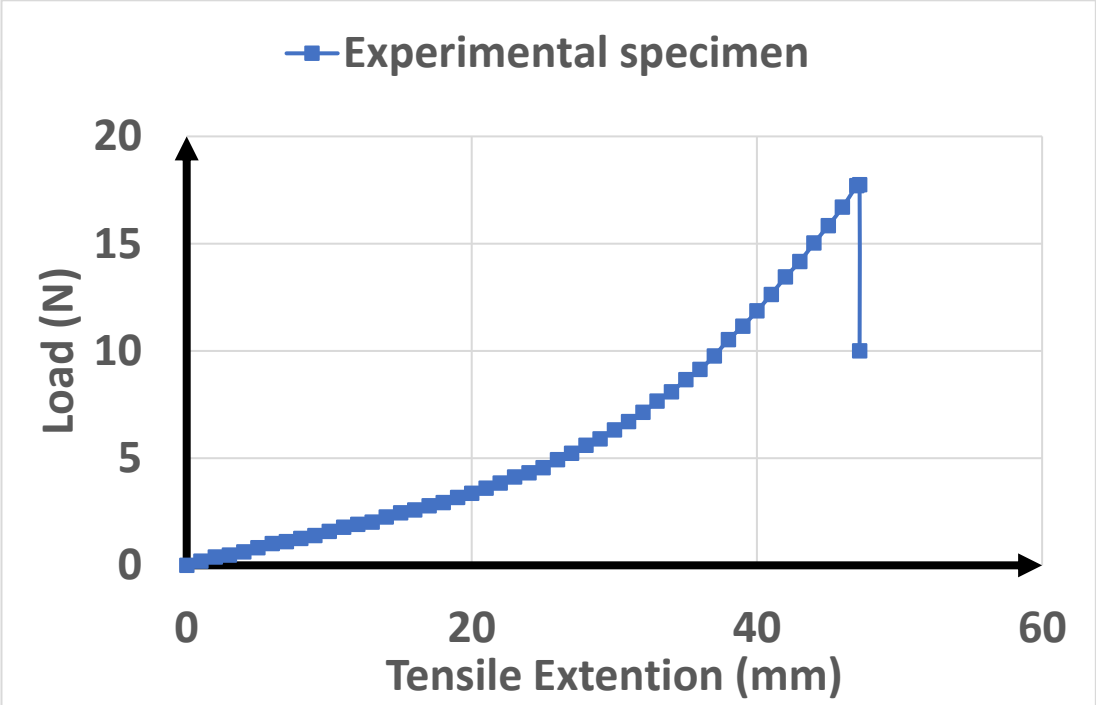

Figure 40: Tensile extension vs load graph for the experimental specimen of 1:10 ratio and a curing time of 4 hours at 60 °C.

CHAPTER IV

RESULTS AND DISCUSSION

4.1 INTRODUCTION

In the previous chapter three material models were presented with the modeling procedure, the modeling was for the membrane and the specimen each of which serves a role in obtaining specific results so a conclusion can be drawn at the end about the following points:

1- Effectiveness of different PDMS to hardener ratios and different material models used on strain and stress with membrane uniformity.
2- Which of the three material models is the most accurate compared to the real experimental values and the effect of constants alteration on the results.

4.2 RATIO AND MATERIAL MODEL EFFECT ON STRAIN AND STRESS VALUES WITH MEMBRANE UNIFORMITY

The difference of PDMS to hardener ratio in the mixture during production has a direct effect on the strain and stress values when the membrane is tested, to know how strain and stress will behave using different mixing ratios all boundary conditions are set the same except for the uniaxial test data mentioned in table 6, each mixing ratio has its corresponding data that will determine material behavior.

Figure 42 and Figure 43 shows the effect of mixing ratios on the strain and stress respectively, the modeling method used is Mooney Rivlin's 5^{th} parameter and the displacement is 10% for all three mixing ratios. Modeling is done as shown in the modeling procedure in the previous chapter. The X axis is the path from the membrane edge to the middle of the membrane, and the Y axis is the strain or stress corresponding to the point located on the membrane as shown in Figure 41.

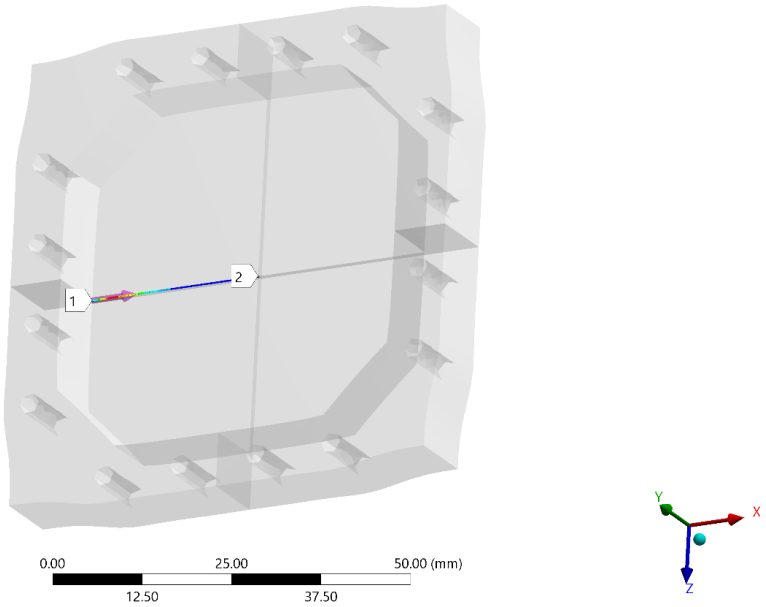

Figure 41: Path taken from point 1 to point 2 for all models to examine stress and strain behavior.

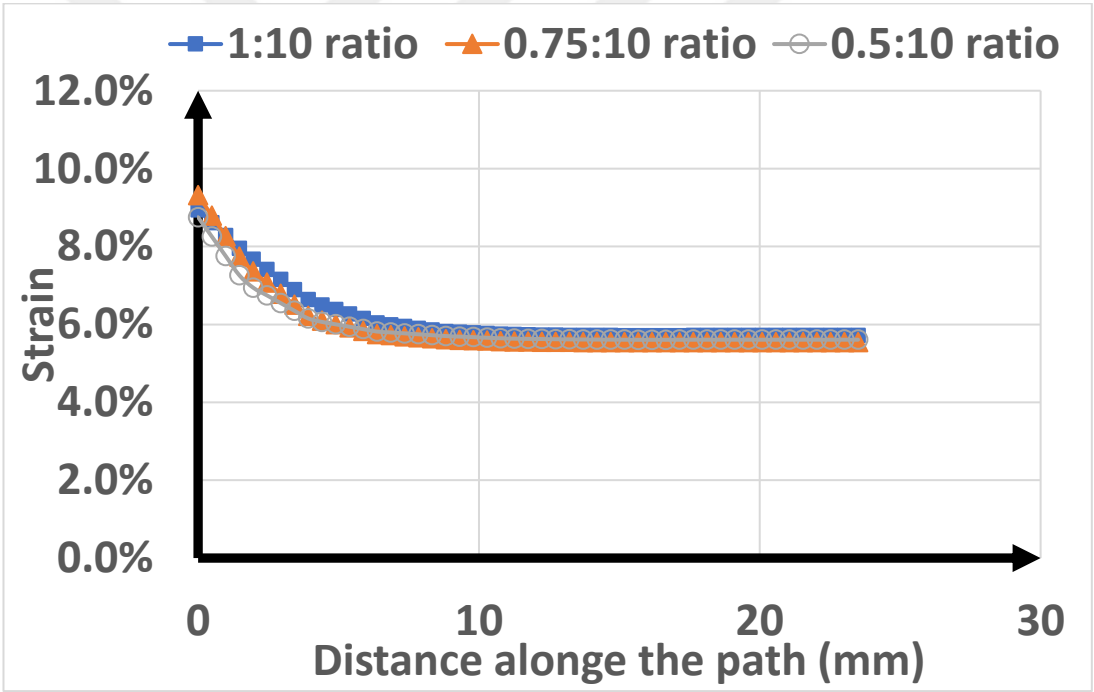

Figure 42: Effect of PDMS to hardener ratio on strain.

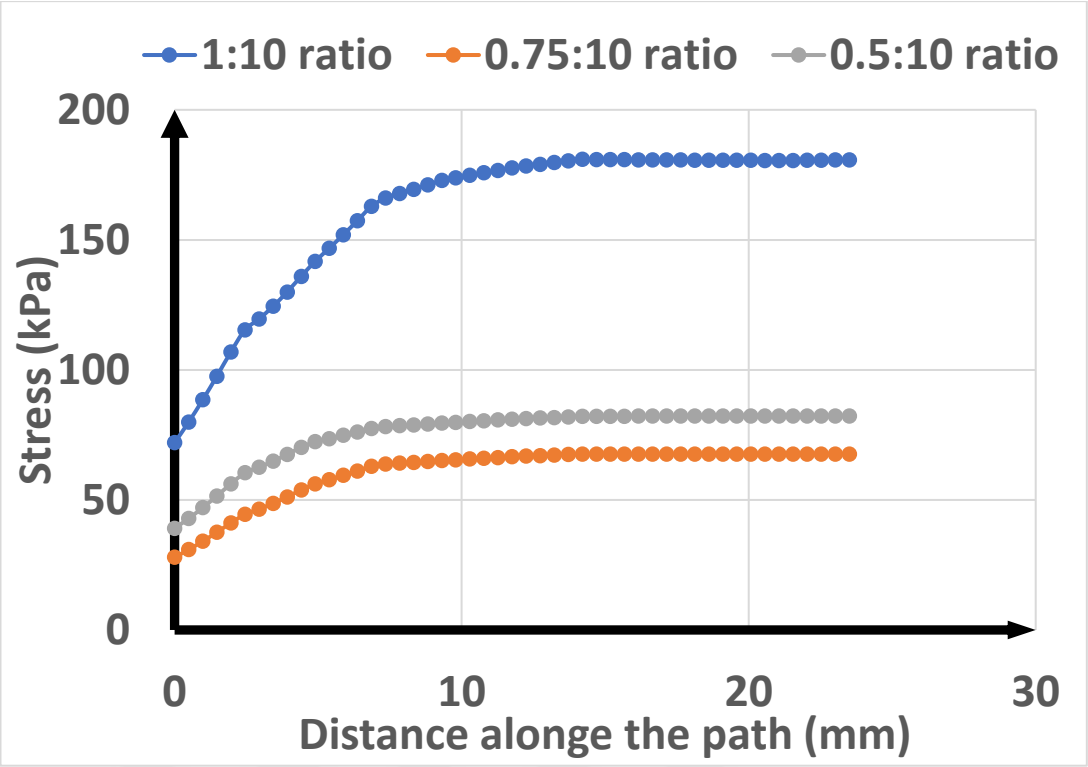

Figure 43: Effect of PDMS to hardener on stress.

Figure 42 shows that a ratio of 1:10 results in a slightly lower value of strain at the beginning then slightly higher than 0.75:10 and 0.5:10 ratios, 10 mm closer to the center it's obvious that strain values are more uniform showing low changes of strain compared to the outer edges of the membrane.

Regarding the stresses, the membrane of the 1:10 ratio examined much higher stress compared to the 0.75:10 and 0.5:10 ratios but all three ratios undergo approximately uniform stress 10 mm from the edge to the center. It's obvious that they follow similar trends but the strain and stress values are different as shown in Figure 43.

Another important factor that affects the strain and stress behavior is the modeling method, to detect the difference between the three modeling methods which are Mooney-Rivlin 5 parameter, Ogden 1st order, and Yeoh 1st order, and how the membrane will deform under these modeling methods the same method used earlier is done, but in this case, the mixing ratio is unified for all three models also the boundary conditions, the only difference will be the model used to simulate the deformation process. Figure 44 and Figure 45 shows the behavior of strain and stress using different material models.

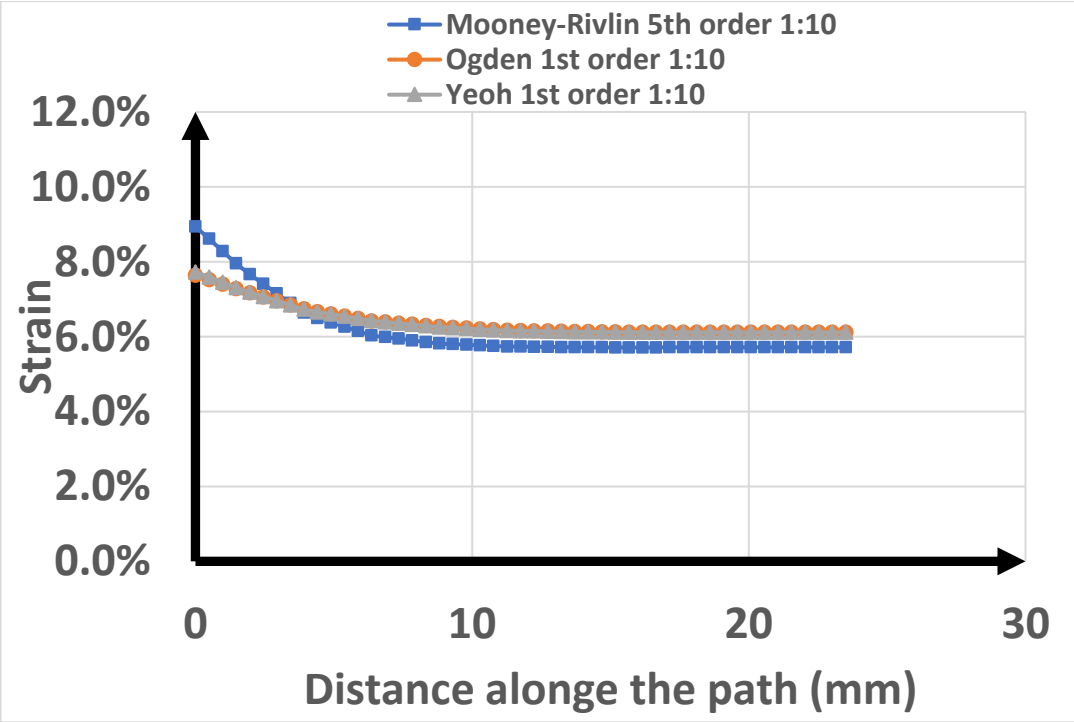

Figure 44: Effect of material model on strain.

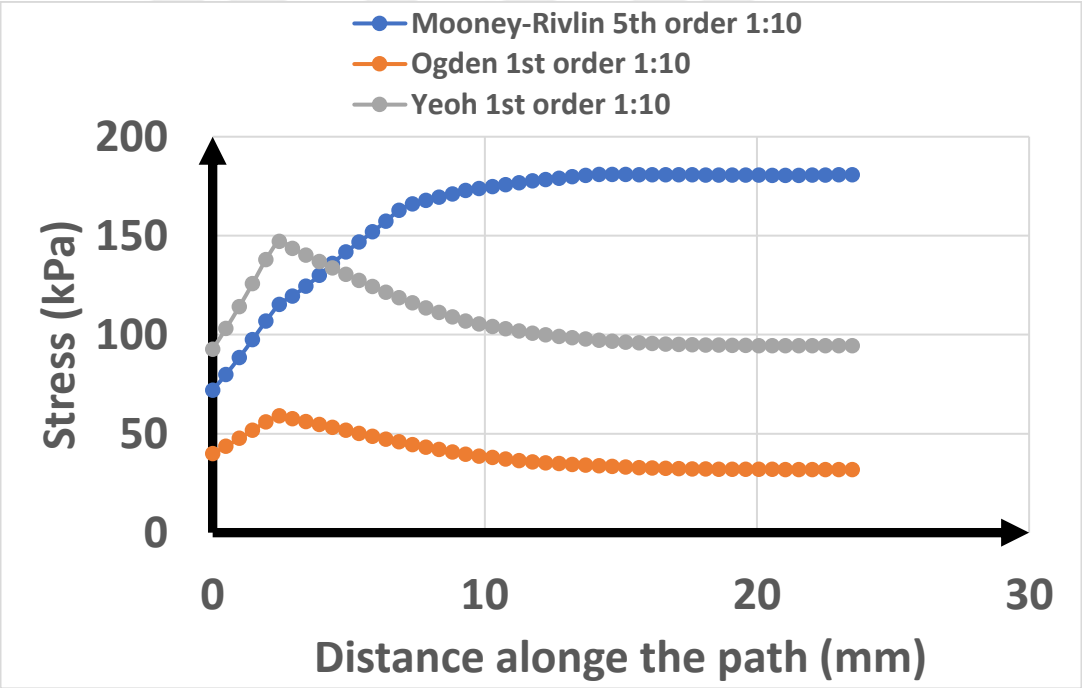

Figure 45: Effect of the material model on stress.

The strain trend for all models is similar except that using Mooney-Rivlin gives higher strain values than the other models at the beginning and slightly lower values approaching the middle with all models tending uniform strain values after 10 mm inwards as shown in Figure 44. On the other hand, stress levels for Ogden and Yeoh material models have the same trend except that the stress values are higher for

the Yeoh material model, but the Mooney-Rivlin model shows a distinct behavior with higher stress levels as shown in Figure 45.

Regarding strain uniformity as mentioned in the previous chapter, the best membrane that passed the tearing test was the membrane with the ratio of 0.75:10, with that being said the strain uniformity of that membrane shown in Figure 46 is calculated to be 0.89, using the most accurate material modeling method Mooney-Rivlin 5^{th} order as stated in the upcoming section 4.3.

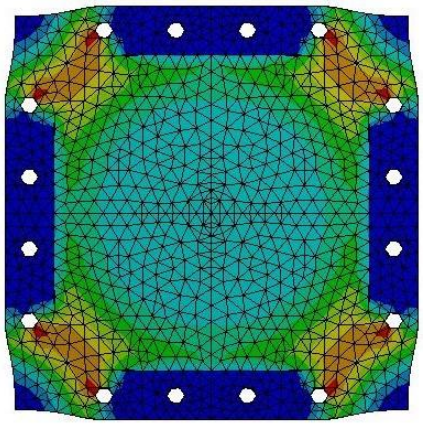

Figure 46: Strain distribution for 0.75:10 ratio membrane using Mooney-Rivlin 5th order material model.

4.3 MATERIAL MODEL ACCURACY AND CONSTANTS EFFECT

To find which material model is the most accurate each model should be compared to real experimental data. Specimens with different production conditions were sent to the METU laboratory to do a tensile test experiment on them, Figure 40 shows the tensile test result for a specimen produced having a ratio of 1:10 and cured for 4 hours at 60 °C.

Now using Ansys, a tensile test is modeled using each of the three models taking into consideration the same conditions of the real specimen, the uniaxial test data used was for 1:10 from table 6. Figure 47 shows each model's results compared to the real specimen.

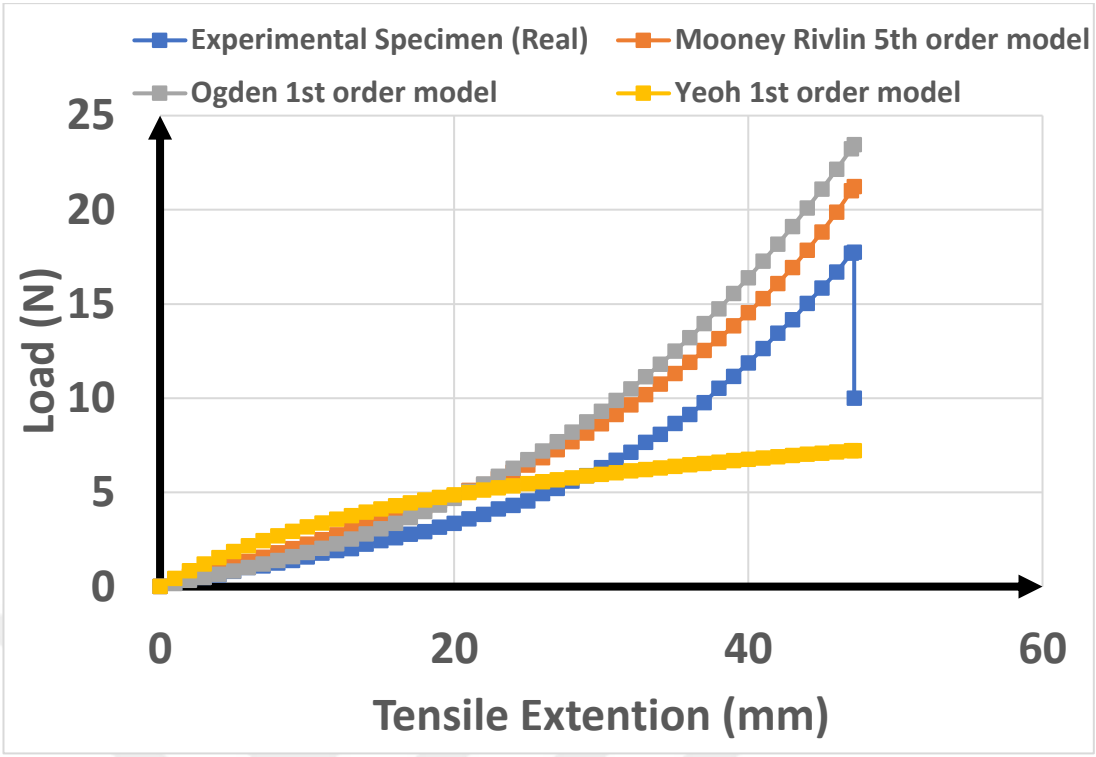

Figure 47: Tensile test data of the real specimen and the three material models (Mooney-Rivlin, Ogden, and Yeoh).

Figure 47 above shows that the Mooney-Rivlin material model gave the most accurate and closest readings to the experimental specimen while Ogden comes second and Yeoh is the furthest with an opposite trend.

Now by altering the material constants of the Mooney-Rivlin material model, it's possible to get more closer to the real values thus a more accurate model. Table 5 below shows the new constants that give a more accurate curve to the experimental specimen.

Table 5: Mooney-Rivlin material model altered constants.

Material Constants	C10	C01	C20	C11	C02
Absolute value decreased by 20% from the default values	-2598216.1	2868348.801	6408704.989	-19350270.	16210152.93

Now by using the new set of constants the tensile test model is solved again giving more accurate curve than the previous default constants model as shown in Figure 48.

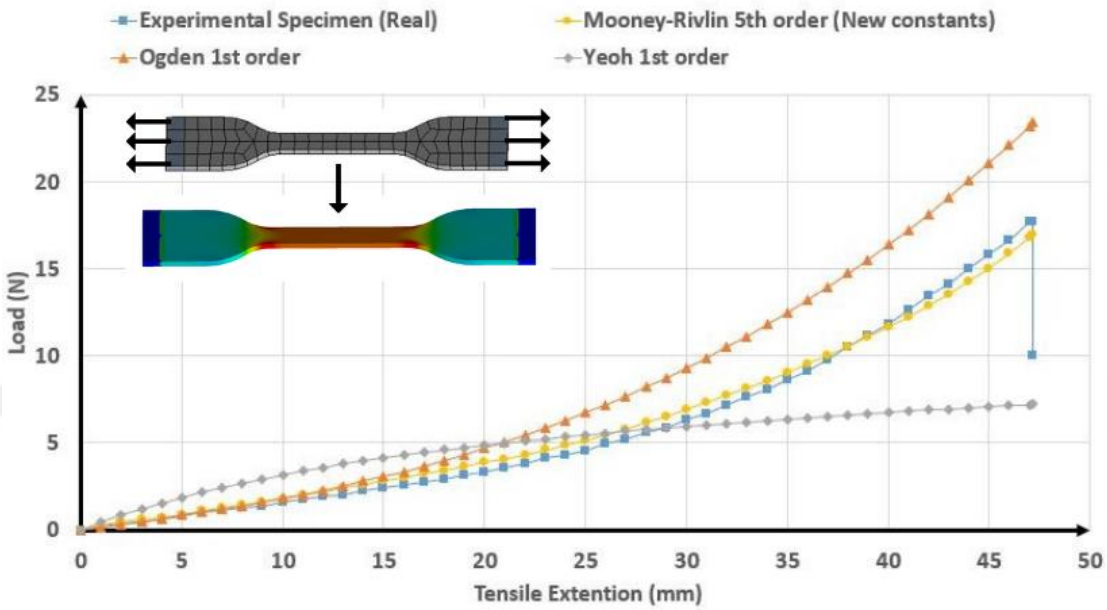

Figure 48: Tensile extension Vs load for different material constants.

CHAPTER V

CONCLUSION

5.1 OUTCOMES

This study addressed the non-uniform strain distribution issue in commercially available membrane-based cell stretching systems. Through finite element analysis, it was determined that the strain distribution in the membranes was significantly non-uniform, which had a negative impact on the reliability and reproducibility of test results. A systematic approach was proposed to overcome this challenge, which involved changing the loading condition by applying displacement to the edges of the membrane instead of pulling from the corners. Modifying the loading conditions resulted in high-stress levels in the membrane, leading to tearing and failure. The membrane shape was optimized to reduce stress intensity by considering three different geometries: a membrane with a circular chamber, a square chamber with rounded corners, and a square chamber with chamfered corners. Also, several hardener-to-PDMS ratio mixtures are examined with different curing conditions to overcome tearing.

The finite element modeling proceeded using three different modeling methods each of these methods gave distinct stress and strain values and behavior, the modeling results are later compared to experimental results, and accordingly, this gave an overview of which of these modeling methods is the most reliable. It is observed that the curve-fitting method used by ANSYS software does not completely match the experimental results. Consequently, the material model is calibrated by a sensitivity analysis method to obtain the best fit. These parameters are used to predict strain distribution in the membrane.

5.2 FUTURE WORK

The field of mechanobiology is wide and open for more work to be done unlike other fields, the work done in this thesis can be expanded and deepened in more. Here are some proposals for the future work in this field:

- The tearing problem in this thesis has been solved by tailoring PDMS material properties. In our finite element models, we didn't include any damage model to predict the failure. Therefore, including damage models to predict failure can be considered important future work for this study.
- A comprehensive material model for the PDMS which also included hardener-to-PDMS ratio, curing time, and temperature is needed to reduce the number of necessary tests to characterize PDMS material.
- The verification of the strain distribution in real-time biaxial cell stretching is also needed by using digital image correlation (DIC) techniques.

REFERENCES

Aydi Ali, Hosseini, M. and Sahari, B. B. (2010), "A Review of Constitutive Models for Rubber-Like Materials", *American J. of Engineering and Applied Sciences*, Vol. 3, No. 1, pp. 232-239.

ASHBY Michael and JONES David (2012), *Engineering materials 1 : an introduction to properties, applications, and design*, Butterworth-Heinemann Publications, USA.

BTH (2014), BTH Report 2014: *In cooperation with Practical implementation of hyperelastic material methods in FEA models*, Blekinge Institute of Technology, Karlskrona.

CHANG Mengzhou, TANG Enling, HAN Yafei, CHEN Chuang, GUO Kai, LIU Chang and WANG Zhenqing (2020), "A parametric analysis of damage evolution for pull-out of a rigid fiber from an elastomer matrix", *Journal of Materials Research and Technology*, Vol. 9, No. 4, pp. 7434-7448.

CHO Han Saem, KIM Hyun A, SEO Dong Woo and JEOUNG Sae Chae (2021), "Poisson's ratio measurement through engraving the grid pattern inside poly (dimethylsiloxane) by ultrafast laser", *Japanese Journal of Applied Physics*, Vol. 60, No. 10, pp. 2-3.

CHO Han Saem, KIM Hyun A, SEO Dong Woo and JEOUNG Sae Chae (2021), "Poisson's ratio measurement through engraving the grid pattern inside poly (dimethylsiloxane) by ultrafast laser", *Japanese Journal of Applied Physics*, Vol. 60, No. 10, pp. 2-3.

IZDIHAR Kamal, RAZAK Hairil Rashmizal Abdul, SUPION Nurzulaikha, KARIM Muhammad Khalis Abdul, OSMAN Nurul Huda and NORKHAIRUNNISA Mazlan (2021), "Structural, mechanical, and dielectric properties of polydimethylsiloxane and silicone elastomer for the fabrication of clinical-grade kidney phantom", *Journal of Applied Sciences*, Vol. 11, No. 3, pp. 1-13.

KAMBLE Harshad, BARTON Matthew J, JUN Myeongjun, PARK Sungsu and NGUYEN Nam-Trung (2016), "Cell stretching devices as research tools: Engineering and biological considerations", *Journal of Lab on a Chip*, Vol. 16, No. 17, pp. 3193-3203.

KHANAFER Khalil, DUPREY Ambroise, SCHLICHT Marty and BERGUER Ramon (2009), "Effects of strain rate, mixing ratio, and stress-strain definition on the mechanical behavior of the polydimethylsiloxane (PDMS) material as related to its biological applications", *Journal of Biomedical Microdevices*, Vol. 11, No. 2, pp. 503-508.

KREUTZER Joose, IKONEN Liisa, HIRVONEN Juha, PEKKANEN-MATTILA Mari, AALTO-SETÄLÄ Katriina and KALLIO Pasi (2014), "Pneumatic cell stretching system for cardiac differentiation and culture", *Journal of Medical Engineering and Physics*, Vol. 36, No. 4, pp. 496-501.

LIU Miao, SUN Jianren, SUN Ying, BOCK Christopher and CHEN Quanfang (2009), "Thickness-dependent mechanical properties of polydimethylsiloxane membranes", *Journal of Micromechanics and Microengineering*, Vol. 19, No. 3, pp. 2-3.

MIRANDA Ines, SOUZA Andrews, SOUSA Paulo, RIBEIRO Joao, CASTANHEIRA Elisabete, LIMA Rui and MINAS Garca (2022), "Properties and applications of PDMS for biomedical engineering: A review", *Journal of Functional Biomaterials*, Vol. 13, No. 1, pp. 1-4.

PHOTHIPHATCHA Jate and PUTTAPITUKPORN Tumrong (2021), "Determination of material parameters of PDMS material models by MATLAB" *Journal of Engineering Journal*, Vol. 25, No. 4, pp. 11–28.

PHOTHIPHATCHA Jate and PUTTAPITUKPORN Tumrong (2021), "Determination of material parameters of PDMS material models by MATLAB" *Journal of Engineering Journal*, Vol. 25, No. 4, pp. 11–28.

RODRIGUES Raquel, PINHO Diana, BENTO David, LIMA Rui and RIBEIRO Joao (2016), "Wall expansion assessment of an intracranial aneurysm model by a 3D Digital Image Correlation System", *Journal of the International Measurement Confederation*, Vol. 88, pp. 262–270, DOI: 10.1016/j.measurement.2016.03.045.

SADEGH-CHERI Mohammad (2019), “Design, Fabrication, and Optical Characterization of a Low-Cost and Open-Source Spin Coater”, *Journal of Chemical Education*, Vol. 96, pp. 1268-1272, DOI: 10.1021/acs.jchemed.9b00013.

SEETHAPATHY Suresh and GÓRECKI Tadeusz (2012), “Applications of polydimethylsiloxane in analytical chemistry: A review”, *Analytica Chimica Acta*, Vol. 750, pp. 48-62, DOI: 10.1016/j.aca.2012.05.004.

SHAO Yue, TAN Xinyu, NOVITSKI Roman, MUQADDAM Mishaal, LIST Paul, WILLIAMSON Laura, FU Jianping and LIU Allen (2013), “Uniaxial cell stretching device for live-cell imaging of mechanosensitive cellular functions”, *Journal of Review of Scientific Instruments*, Vol. 84, No. 11, DOI: 10.1063/1.4832977.

VICTOR Andrews, RIBEIRO Joao and ARAÚJO Fernando (2019), “Study of PDMS characterization and its applications in biomedicine: A review”, *Journal of Mechanical Engineering and Biomechanics*, Vol. 4, No. 1, pp. 1-9.

WANG Zhixin, VOLINSKY Alex and GALLANT Nathan (2014), “Crosslinking effect on polydimethylsiloxane elastic modulus measured by custom-built compression instrument”, *Journal of Applied Polymer Science*, Vol. 131, No. 22, DOI: 10.1002/app.41050.

WPI (2019), *WPI Report 2019: Development of Microscope Stage BioStretch Device for Mechanobiology*, Worcester Polytechnic Institute, Worcester.

WPI (2019), *WPI Report 2019: Development of Microscope Stage BioStretch Device for Mechanobiology*, Worcester Polytechnic Institute, Worcester.

APPENDECIES

APPENDIX A: TABLES

Table 6: Stress-strain values extracted from figure 36.

PDMS/Hardener (1:10)		**PDMS/Hardener (0.75:10)**		**PDMS/Hardener (0.5:10)**	
X-Axis Strain	Y-Axis Stress (MPA)	X-Axis Strain	Y-Axis Stress (MPA)	X-Axis Strain	Y-Axis Stress (MPA)
0.049006767	0.058939096	0.003261553	0.029469548	0	0.029411765
0.091484007	0.088408644	0.088228874	0.029469548	0.101472995	0.057331279
0.133954826	0.147347741	0.1699218	0.058939096	0.196399345	0.055935304
0.176432066	0.176817289	0.241810804	0.088408644	0.281505728	0.054683739
0.215634911	0.235756385	0.313706229	0.088408644	0.360065466	0.053528449
0.254837757	0.294695481	0.379059286	0.117878193	0.43207856	0.081881198
0.290779049	0.324165029	0.441144369	0.147347741	0.500818331	0.080870319
0.323445947	0.383104126	0.495059517	0.176817289	0.566284779	0.109319341
0.359380818	0.442043222	0.548974665	0.206286837	0.62193126	0.108501011
0.388779742	0.500982318	0.601255826	0.235756385	0.684124386	0.107586406
0.424714614	0.559921415	0.653530567	0.294695481	0.736497545	0.106816213
0.454113538	0.618860511	0.696007807	0.324165029	0.785597381	0.106094156
0.486780436	0.677799607	0.741753021	0.353634578	0.831423895	0.105420237
0.512904966	0.766208251	0.787498234	0.383104126	0.880523732	0.134109945
0.539029495	0.854616896	0.826713921	0.383104126	0.923076923	0.133484163
0.565160445	0.913555992	0.862648792	0.442043222	0.965630115	0.162270145
0.594552949	1.001964637	0.901851638	0.500982318	1.008183306	0.161644363
0.620677479	1.090373281	0.941060904	0.530451866	1.044189853	0.161114855
0.643534034	1.178781925	0.973734222	0.559921415	1.083469722	0.189948975
0.669652144	1.296660118	1.00640112	0.618860511	1.119476268	0.218831231
0.692495859	1.444007859	1.042342412	0.648330059	1.155482815	0.218301723
0.715345994	1.561886051	1.071741336	0.707269155	1.188216039	0.217820352
0.741464104	1.679764244	1.101133839	0.7956778	1.220949264	0.246750746
0.764307819	1.827111984	1.133800737	0.854616896	1.253682488	0.246269375
0.78388356	1.974459725	1.163199661	0.913555992	1.281505728	0.275271975
0.806720855	2.151277014	1.192598585	0.972495088	1.312602291	0.304226437
0.826283755	2.357563851	1.218729535	1.031434185	1.342062193	0.303793203
0.84912105	2.534381139	1.244860485	1.090373281	1.371522095	0.332771734
0.86867753	2.770137525	1.267717041	1.178781925	1.397708674	0.361798402
0.88823401	3.00589391	1.293847991	1.237721022	1.420621931	0.361461442

Table 6 Continued

0.90779049	3.241650295	1.319972521	1.326129666	1.450081833	0.419851738
0.927334129	3.536345776	1.342822656	1.444007859	1.47299509	0.448926543
0.946871348	3.860510806	1.368947186	1.532416503	1.499181669	0.477953211
0.963140594	4.184675835	1.391797321	1.650294695	1.522094926	0.507028016
0.981037405	4.538310413	1.414653877	1.73870334	1.545008183	0.536102821
1.00218935	4.950884086	1.434236039	1.856581532	1.56792144	0.565177626
1.018432913	5.392927308	1.457079754	2.003929273	1.590834697	0.594252431
1.034670057	5.864440079	1.479923469	2.151277014	1.613747954	0.623327236
1.052537977	6.350687623	1.499505631	2.269155206	1.633387889	0.652450178
1.067118661	6.925343811	1.520712149	2.431237721	1.653027823	0.710984885
1.081705767	7.470530452	1.541912246	2.622789784	1.67594108	0.769471455
1.099541585	8.104125737	1.558213593	2.799607073	1.695581015	0.798594397
1.112472232	8.752455796	1.577776494	3.00589391	1.715220949	0.857129104
1.128664432	9.430255403	1.597345815	3.182711198	1.734860884	0.915663811
1.143203385	10.19646365	1.616908715	3.388998035	1.754500818	0.944786753
1.161016732	10.93320236	1.633203642	3.595284872	1.774140753	0.973909695
1.173918487	11.71414538	1.649485727	3.860510806	1.793780687	1.032444402
1.188447809	12.52455796	1.669042208	4.096267191	1.813420622	1.090979109
1.204611118	13.33497053	1.685330714	4.332023576	1.826513912	1.14961009
Null	Null	1.70161922	4.567779961	1.842880524	1.208192933

APPENDIX B: FEA MODELING PROCEDURE

Figure 49: (a) Analysis system selection (b) Engineering data (c) Assign material (d) Insert uniaxial test data to material (e) Uniaxial test data and its stress-strain graph.

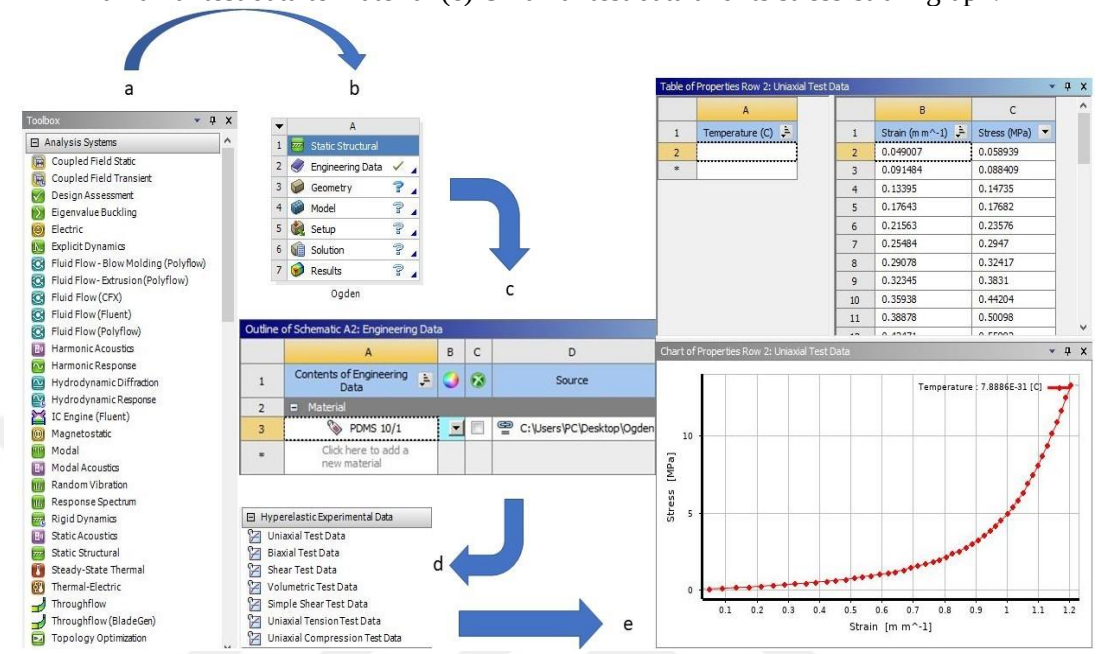

Figure 50: (a) Hyper elastic model selection (b) Solve curve fit (c) Copy calculated values to property (d) Assign incompressibility parameter.

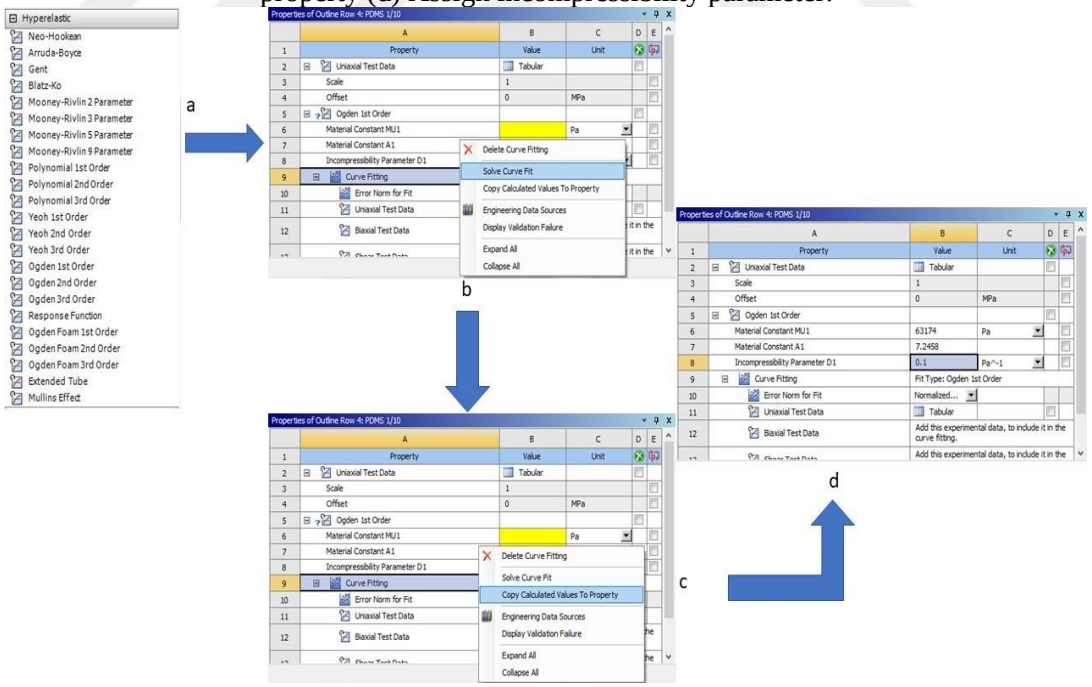

Figure 51: (a) Import geometry (b) Edit geometry in design modeler (c) Generate geometry (d) Geometry generated.

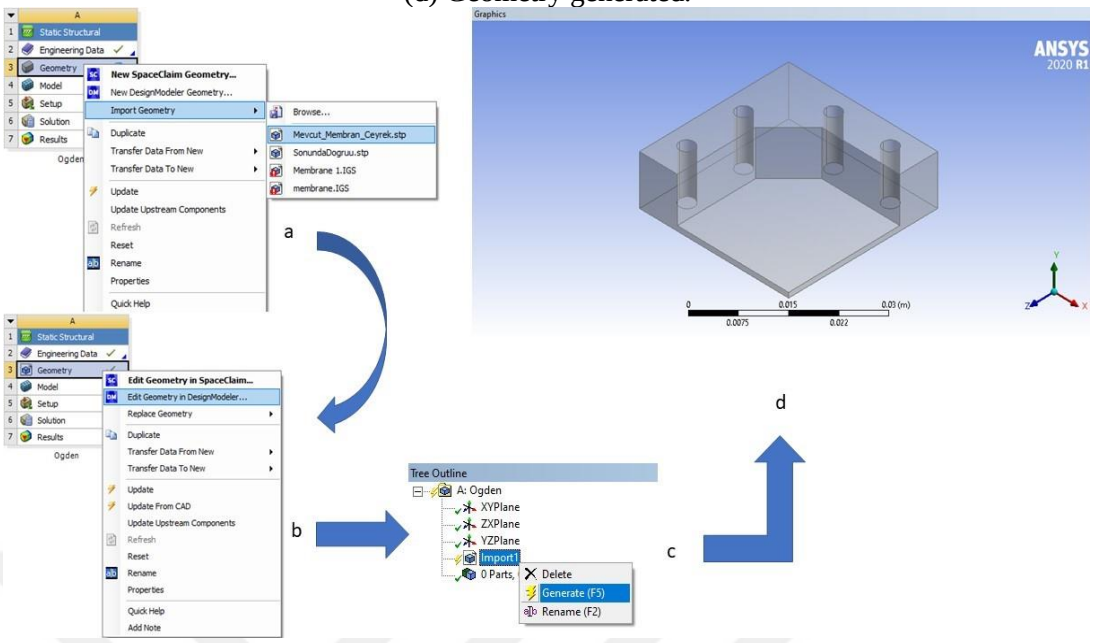

Figure 52: (a) Edit model (b) Select model material.

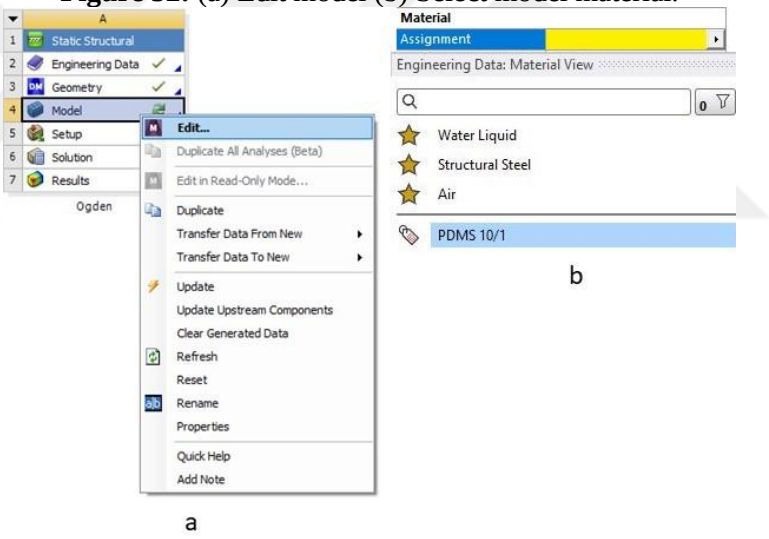

Figure 53: (a) Insert symmetry and assign symmetry region (b) Select faces (c) Insert details of symmetry.

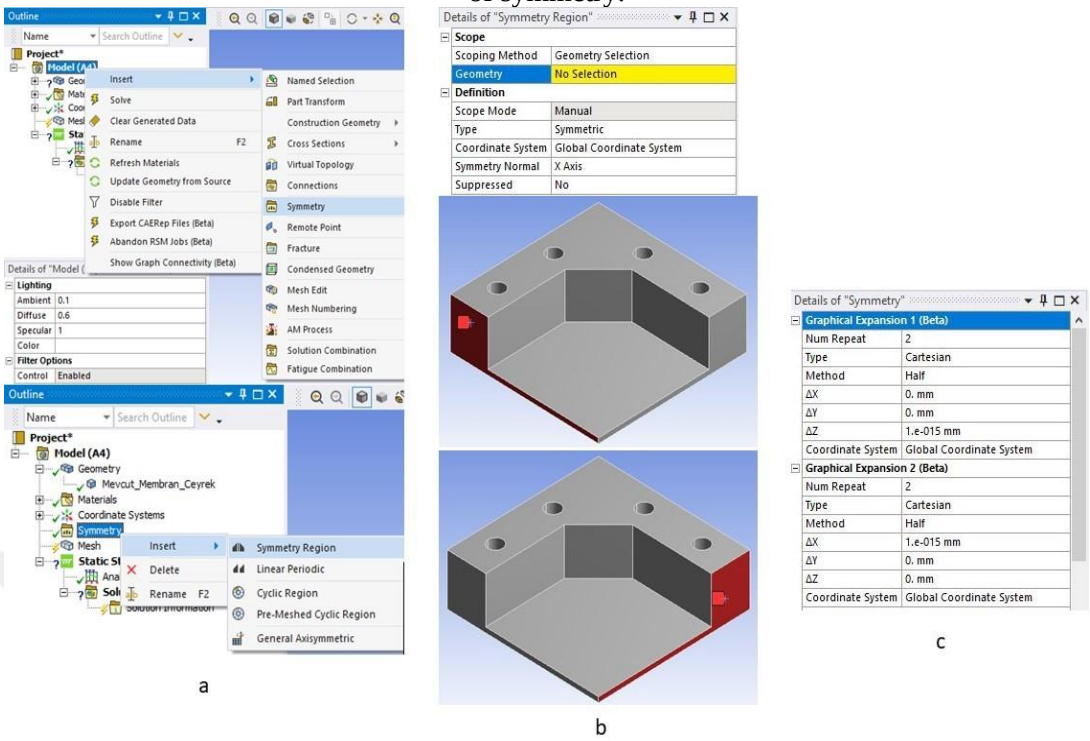

Figure 54: (a) Generate mesh (b) Insert details of analysis settings.

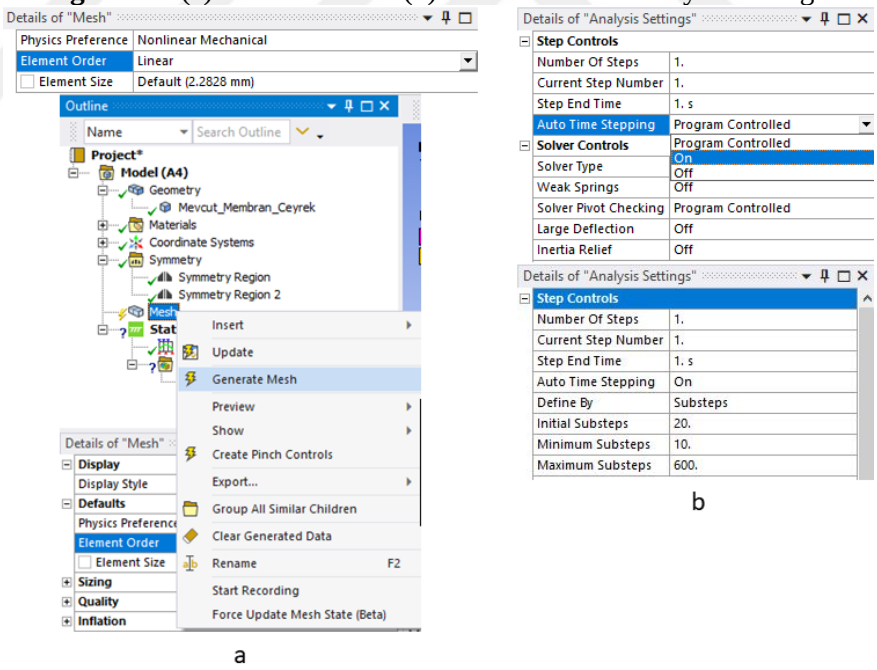

Figure 55: (a) Insert displacement (b) Assign displacement and values to Z axis holes (c) Assign displacement and values to X axis holes.

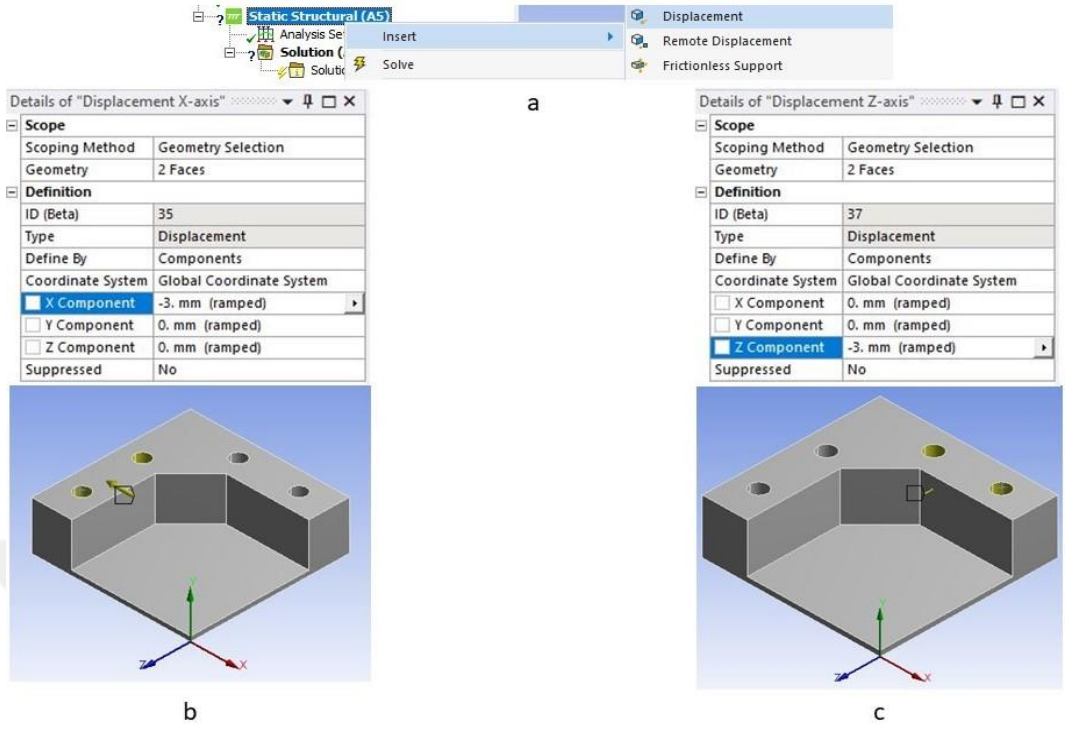

Figure 56: (a) Fix motion on Y axis and keep it free on X and Z axis for all faces (b) Assign displacement and values to the Z axis symmetry face (c) Assign displacement and values to the X axis symmetry face.

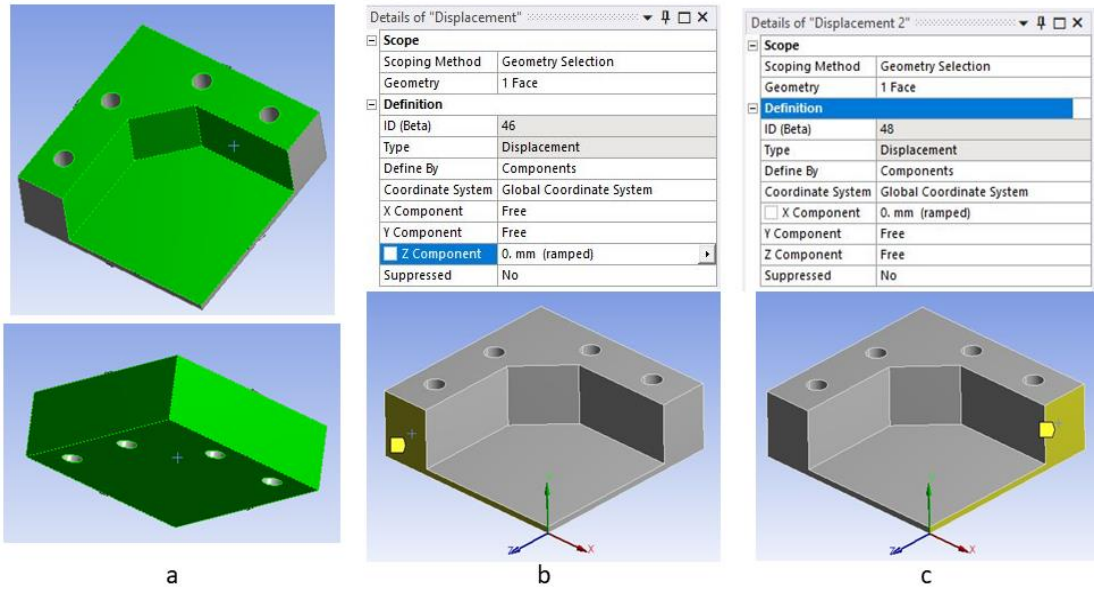

Figure 57: Turn large deflection on.

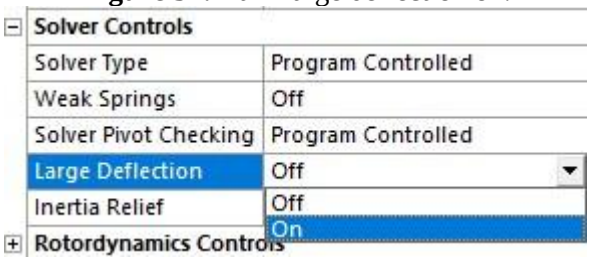

Figure 58: (a) Insert Path (b) Select "Path Type" as two points (c) Start and end points coordinates (d) Path selected.

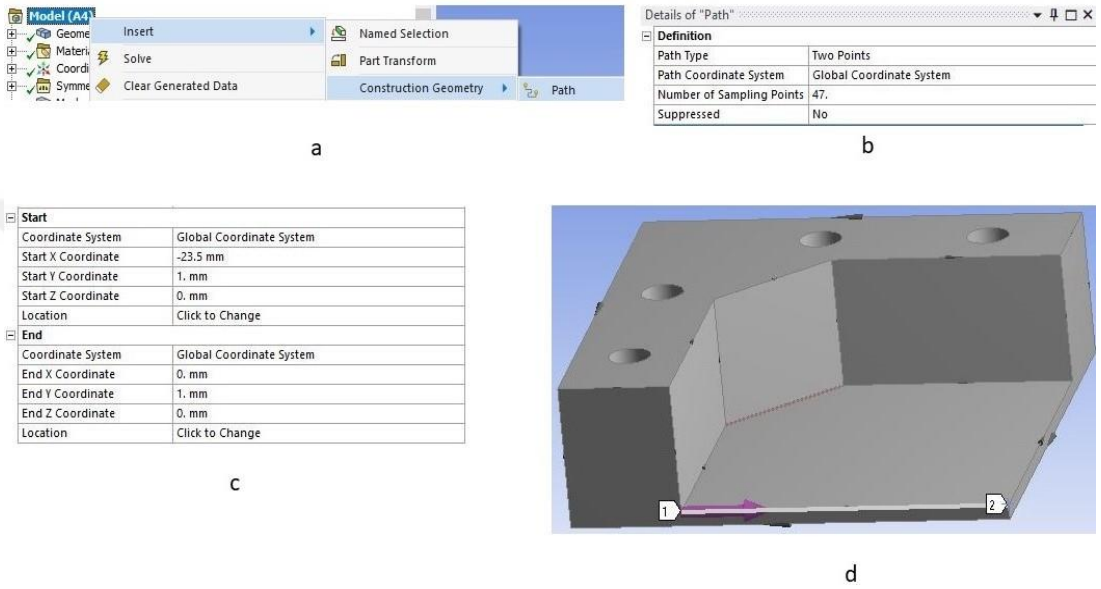

Figure 59: (a) Select Equivalent von-Mises strain (b) Select scoping method as the Path and select the path (c) Evaluate all results.

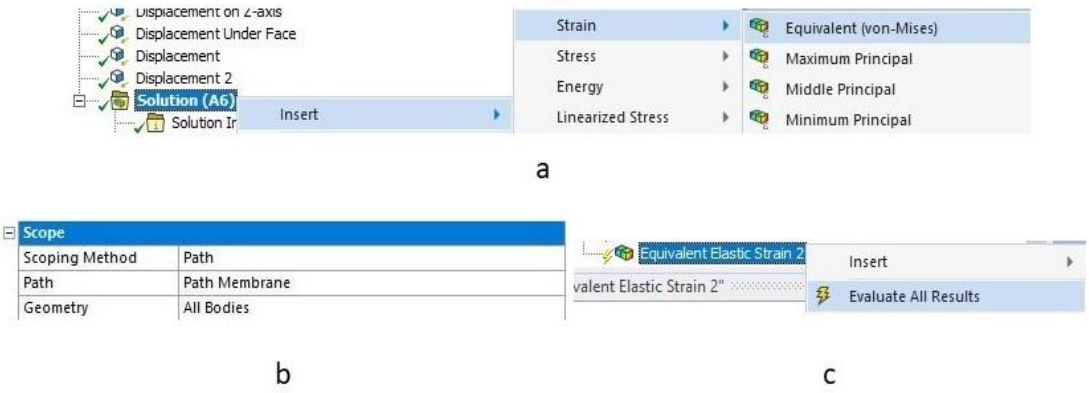

APPENDIX C: ENGINEERING DRAWINGS

Figure 60: PDMS membrane engineering drawing.

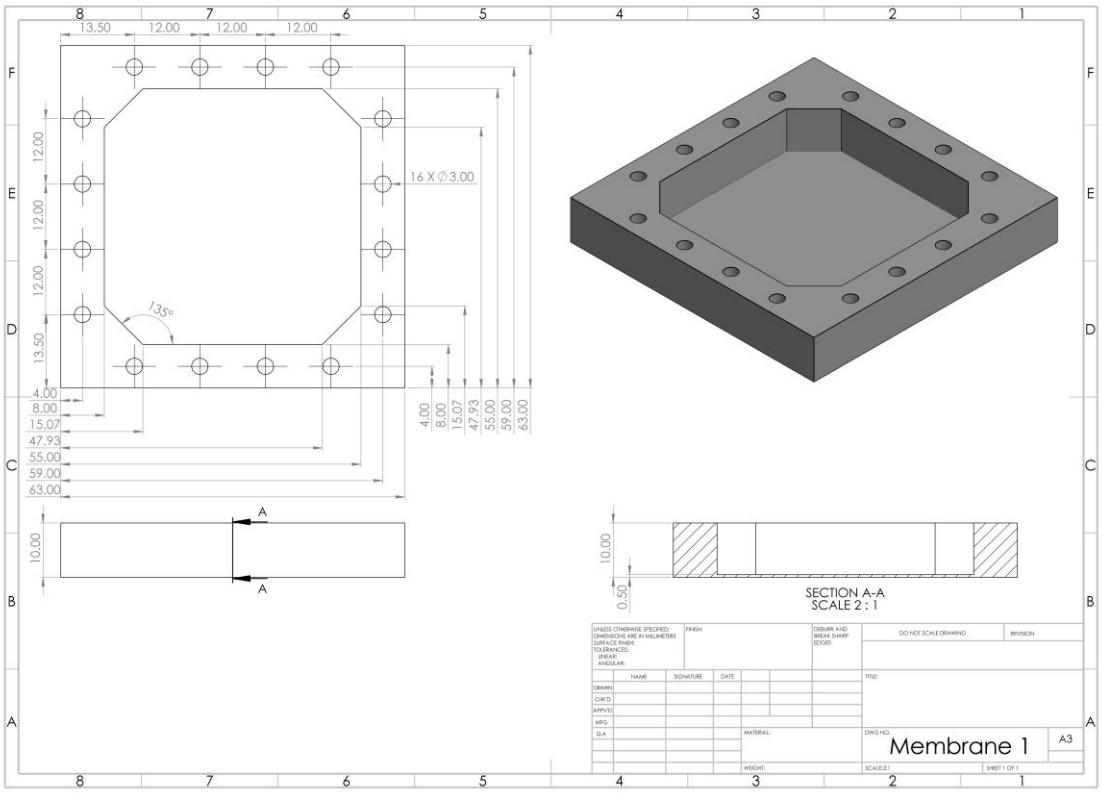

Figure 61: PDMS membrane mold base engineering drawing.

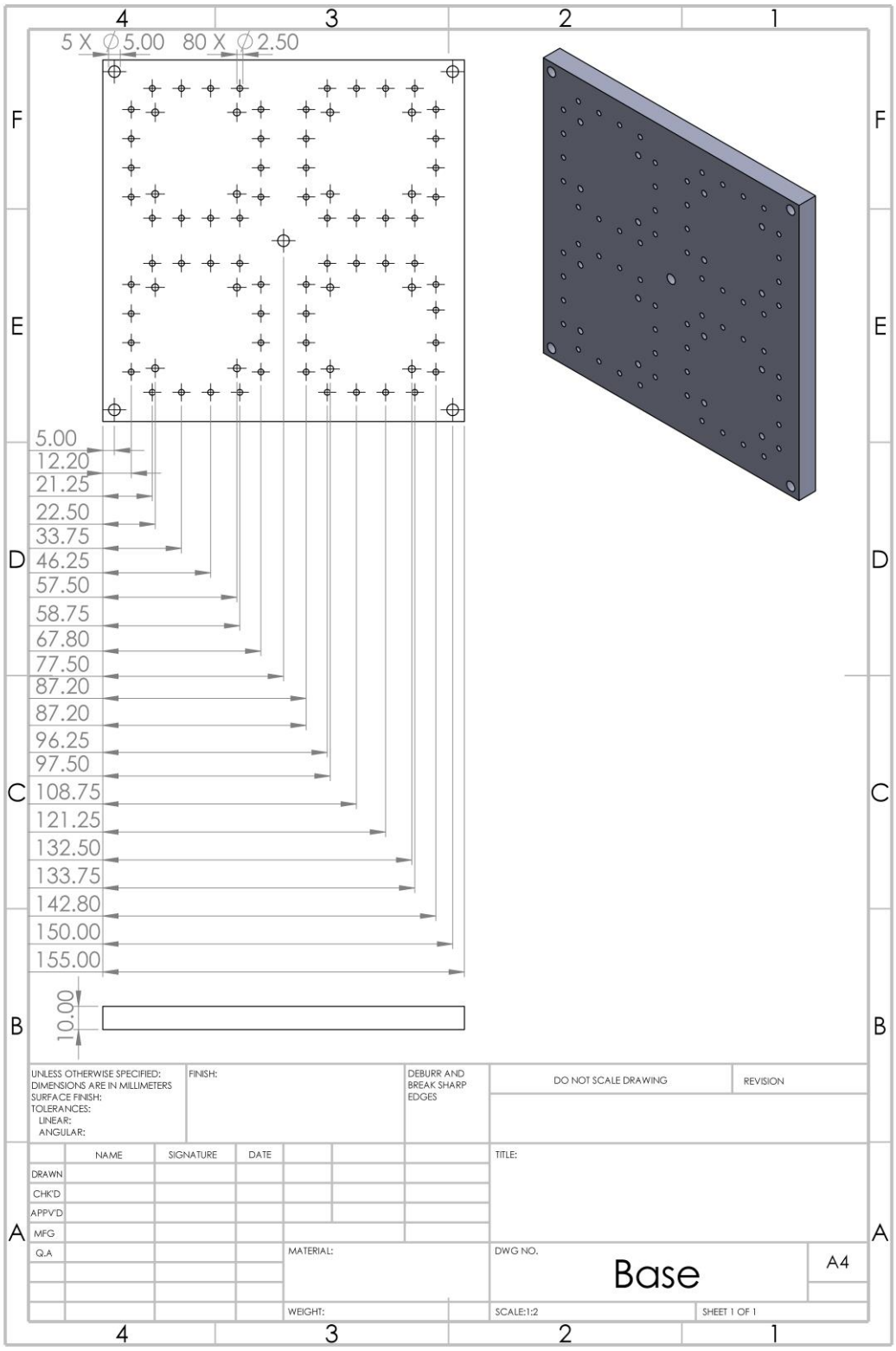

Figure 62: PDMS membrane mold cover engineering drawing.

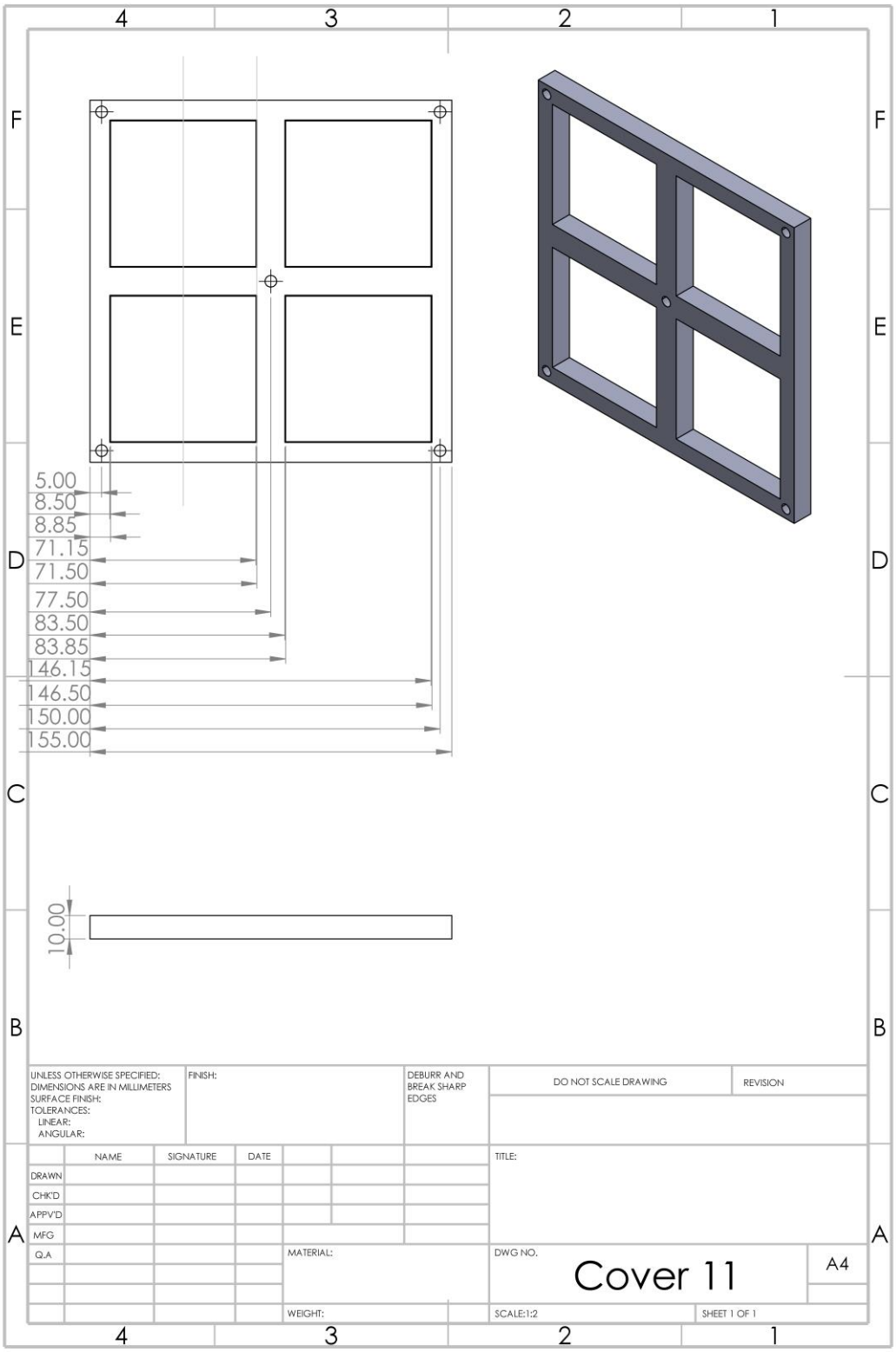

Figure 63: PDMS membrane core mold engineering drawing.

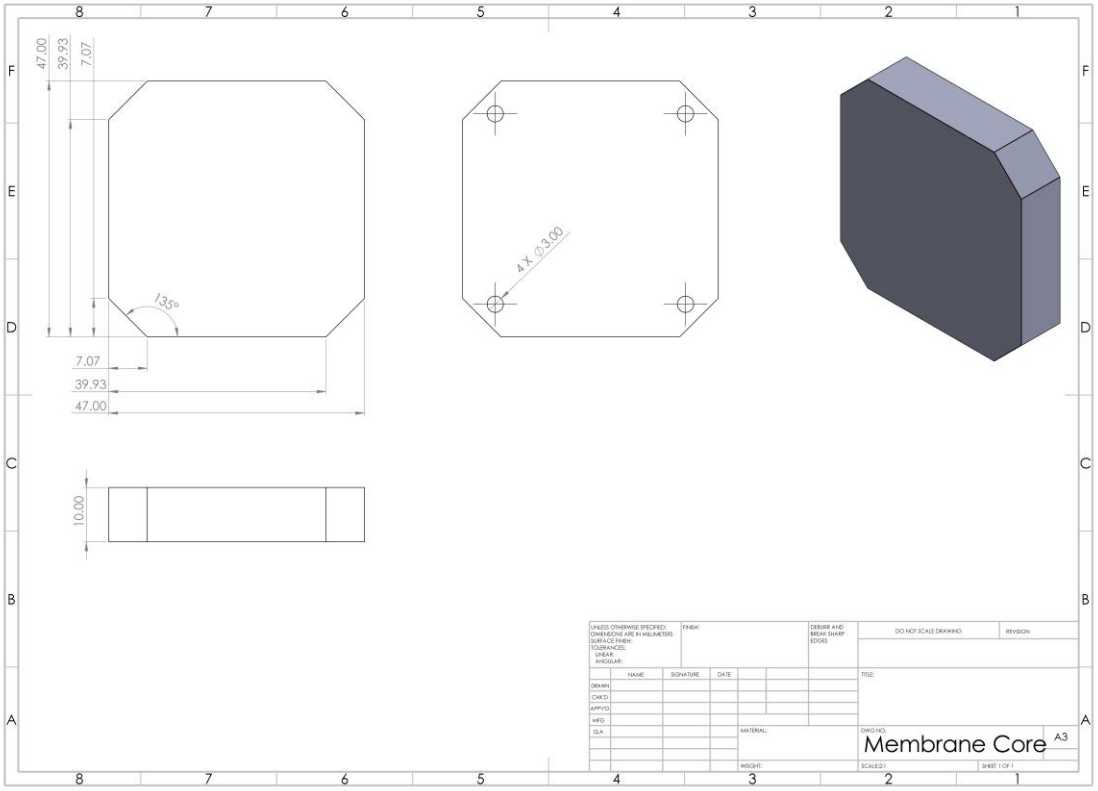

Figure 64: PDMS specimen mold engineering drawing.

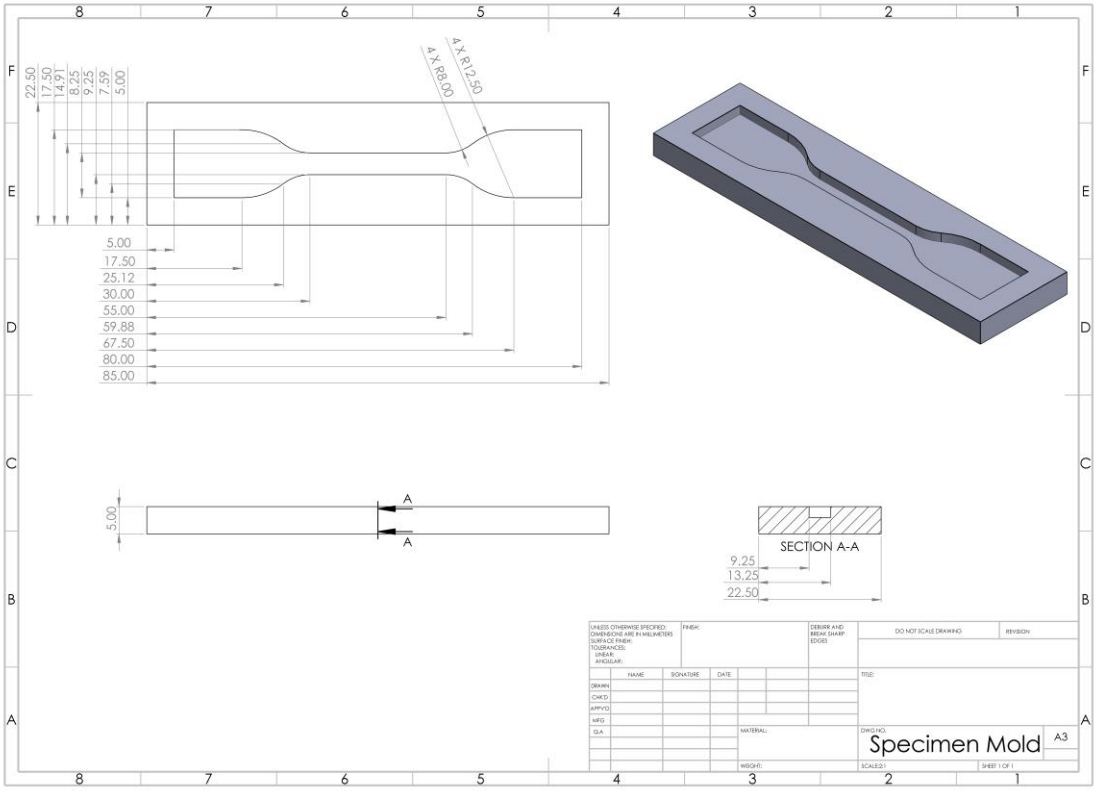

Figure 65: PDMS specimen engineering drawing.